# Numerical Modelling of Tidal Notch Sequences on Rocky Coasts of the Mediterranean Basin

**S. Schneiderwind[1*], S. J. Boulton[2], I. Papanikolaou[3], M. Kázmér[4a], and K. Reicherter[1]**

[1]Institute of Neotectonics and Natural Hazards, RWTH Aachen University, Lochnerstraße 4-20, 52056 Aachen, Germany.

[2]School of Geography, Earth and Environmental Sciences, Plymouth University, Plymouth, Devon PL4 8AA, UK.

[3]Laboratory Mineralogy – Geology, Agricultural University of Athens, Iera Odos 75, 11855 Athens, Greece.

[4]Department of Palaeontology, Eötvös University, H-1117 Budapest, Pázmány Péter sétány 1/c, Hungary.

*Corresponding author: Sascha Schneiderwind (s.schneiderwind@nug.rwth-aachen.de)

[a]Now at: MTA-ELTE Geological, Geophysical and Space Science Research Group, Pázmány Péter sétány 1/c, H-1117 Budapest, Hungary.

**Key Points:**

- Tidal notch modelling incorporating Holocene sea-level, erosion rates, and landmass movement
- Optically emphasized morphological consequences of biasing slow and rapid coastal displacements
- Resulting notch sequences do not necessarily link to certain seismic events and are not chronologically sorted



This article has been accepted for publication and undergone full peer review but has not been through the copyediting, typesetting, pagination and proofreading process which may lead to differences between this version and the Version of Record. Please cite this article as doi: 10.1002/2016JF004132

**Abstract**

Tidal notches have had the potential to form at sea-level from ~6.5 kyr BP in the Mediterranean basin and preserve a symmetrical shape comparable to a quadric polynomial. Continuous erosion, predominantly by biological agents, affects a limestone cliff face from low- to high-tide level at <1 mm/yr. Statically determined, the roots of a quadric polynomial are defined by the tidal range representing the limits of effective erosion. However, gradual variations of eustatic sea-level rise (slow) and coseismic uplift/subsidence (fast) in tectonically active regions contribute to vertical shifts in the erosional base at coastlines. As a consequence, the cliff morphology gets modified through time resulting in widening, deepening and separation of notches and possible overprinting of older features. In order to investigate successive modifications of coastal cliff morphology, we developed a numerical model that considers the erosion rate, the erosion zone relative to sea-level, the regional sea-level curve, and tectonic motion. The results show how slow and rapid sea-level change bias the modern cliff face, and highlight that the present-day notch sequence from top descending to sea-level is not inevitably of decreasing age. Furthermore, the initiation of notch formation is not necessarily linked to the date of a certain seismic event. Especially in extensional tectonic settings where coseismic uplift is low and coastal morphological marks are not as distinct, knowledge about coastal evolution is beneficial for paleoseismological research.

## 1 Introduction

Tidal notches are a generally accepted sea-level marker [e.g. *Pirazzoli et al.*, 1982, 1989, 1991; *Laborel et al.*, 1999; *Kershaw & Guo*, 2001; *Evelpidou et al.*, 2011a,b, 2012a,b; *Boulton & Stewart*, 2015; *Antonioli et al.*, 2015]. Ongoing horizontal erosion of chemical, physical, and biological agents [e.g. *Furlani et al.*, 2011; *Antonioli et al.*, 2015; *Evelpidou & Pirazzoli*, 2016] contributes to notch formation at mean sea-level. As a result, obvious ecological and morphological topographies that range from a few centimeters up to several meters deep occur predominantly on limestone coastlines where tidal ranges are low and erosional processes are concentrated into a narrow vertical range of elevation [*Pirazzoli*, 1986]. It is generally assumed, when these features are raised or submerged from present-day sea-level, that paleo-historic tectonic activity can be inferred from obtained sequences. In particular, tidal notches along coasts of the Mediterranean Sea have been an important marker of coastal tectonism determining rates of Holocene tectonic uplift [e.g. *Pirazzoli et al.*, 1982, 1989, 1991, 1994, *Stewart & Vita-Finzi*, 1996; *Rust & Kershaw*, 2000; *Kershaw & Guo*, 2001; *Evelpidou et al.*, 2012a, *Antonioli et al.*, 2015; *Goodman-Tchernov & Katz*, 2015] (Fig. 1). However, it remains unclear as to what present morphologies can reveal regarding the paleomagnitudes and coseismic uplift of historic earthquakes. It is generally assumed that tidal notches form during relative sea-level stagnation; when vertical land movements and eustatic trends are unison. The database of *Boulton & Stewart* [2015] demonstrated that the formation of tidal notches is not linked to periods of stable or unstable climates in the past, rather it is likely that tectonic activity and earthquake clustering control the spatial and temporal distribution of tidal notches. Only rapid offset between the strandline and erosional base can initiate new notch generation. Thus, the distinction between surface displacement potential in compressional and extensional tectonic settings is absolutely essential [*Schneiderwind et al.*, 2017]. Yet, coseismic offsets on normal faults are at least an order of magnitude smaller than those from thrusting events. However, the misconception that multiple and stacked notches are evidence for meter-scale coseismic events produced by normal faulting still persists [e.g. *Stewart & Vita-Finzi*, 1996]. Therefore, *Cooper et al.* [2007] suggest a different mechanism to explain the occurrence of meter-scale shoreline displacements along normal faults, proposing that individual notches formed when stable climate facilitated sustained erosion and post-glacial sea-level rise became outpaced by the coastal uplift rate. Contrasting this suggestion, *Boulton & Stewart* [2015] argue that this hypothesis does not seem to be the case for the Mediterranean and conclude that notch genesis is dominantly controlled by earthquake clustering.

Only a few attempts to model tidal notch formation have been undertaken. Conceptual notch formation is understood as a reflection of normal distributed erosional potential resulting in a symmetrical shape with the retreat zone of maximum convexity at mean sea-level. *Pirazzoli* [1986] developed the generally accepted idea of a symmetrical V-/U-shaped notch profile on a sheltered cliff where the floor extends to the limit of permanent immersion at tidal low stand, and the roof marks the upper limit of frequent high tides. The maximum retreat point is located near mean sea-level. Gradual relative sea-level change may produce a variety of tidal notch profiles. *Evelpidou et al.* [2011a,b] provided a set of graphic schemes of tidal notch profiles resulting from different combinations of relative sea-level changes. In general, the authors pointed out, that relative sea-level stability deepens the notch whereas gradual sea-level change widens the morphological incision. Furthermore, rapid sea-level changes can be divided into two categories. Firstly, where rapid relative movements greater than the tidal range result in notch formation while the former notch remains preserved, and secondly rapid displacements smaller than the tidal range that produce notch profiles with

two closely located vertices separated by a small protrusion in between. In other words, the pre-existing morphology is modified due to overlapping erosional zones prior to and after the displacement [see also *Pirazzoli*, 1986; *Evelpidou et al.*, 2012a]. Notch profile modification is also a product of increasing exposure to wave action. Other than bioerosive agents, cliff quarrying by wave action is generally not considered in tidal notch development. It is generally assumed that quarrying is insignificant for sheltered exposures [*Pirazzoli*, 1986; *Antonioli et al.*, 2015]. However, *Larson et al.* [2011] introduced an analytical, yet physically based, model that considers wave impacts on coastal dunes and cliffs from laboratory experiments. Their results show complex feedbacks in cliff notch evolution when nearby beaches provide sediments that increase the erosive capacity of impacting waves. A third approach is presented by *Trenhaile* [2014] focusing on notch formation by tidal wetting and drying cycles and salt weathering. Here, notch profiles were produced within the 3,000-6,000 year period of constant relative sea-level. As a result of ongoing erosion affecting the same cliff section, several iterative cliff collapses were generated. Wetting and drying cycles as well as salt weathering attain importance especially when saline water penetrates into structural discontinuities of the bedrock. Evaporation processes and subsequent cumulative deposition of salt crystals trigger fragmentation of the rock and result in geomorphic modifications. A similar process occurs owing to frost weathering in cold climates [*Trenhaile & Mercan*, 1984]. By applying a gridded mathematical model *Trenhaile* [2016] suggests for limestone notch profiles in the Mediterranean that notch morphology is the product of a variety of local- (e.g. cliff slope and bed resistance to erosion) and regional-scale (e.g. varying erosional efficacy) factors. By adding a wide range of different variables (e.g. variable slope gradient and notch collapse on a local scale and general influence of sea-level changes on a regional scale) a theoretical approach is provided suggesting that similar profiles can be produced by different combinations of applied parameters.

Except for the work of Trenhaile [2015], all previous notch models do not address actual changing glacio-hydro-isostatic conditions during the Holocene. Although previous studies generally consider changing sea-levels, both rapid and gradual, unlocking the temporal interplay between sea-level change causative factors has not yet been deeply investigated. However, considering actual and region-specific parameters enhances the understanding of the development of paleoshorelines and their deformation by active tectonics particularly for paleoseismological studies. Therefore, previous models are herein described as static (theoretical) models. In order to visualize the development of notch sequences incorporating eustatic and isostatic balances, erosion rates, coseismic uplift, and cliff steepness, we present a simple numerical model that simulates the migration of the erosional base through the Holocene. Furthermore, local sea-level curves and coastal uplift rates for eight regions across the Mediterranean Basin act as input parameters in order to verify potentials of notch formation and associated theoretical paleoseismological significance when earthquake activity is introduced as well. Both slow and rapid relative landmass displacements interplay through time causing overprinting and modification of pre-existing notch generations. As the first application in this manner, the time-sliced visualization enables researchers to have an enhanced understanding of tidal notch sequence evolution, and thus better interpretations of co-seismic sequences on tectonic coasts.

## 2 Contributors to notch sequencing

The term tidal notch refers to a horizontal erosion feature at sea-level [*Kelletat*, 2005b] due to the coeval action [*Antonioli et al.*, 2015] of biological, chemical, and physical factors [*Pirazzoli*, 1986]. It should be noted that the ratio between erosional components has

not been discovered so far. *Pirazzoli & Evelpidou* [2013] consider only tidal notches that exclusively formed by bioerosional processes in sheltered places, and other workers have similarly concluded that biological mechanisms at least dominate notch forming erosion potentials [*Evelpidou et al.*, 2012b; *Antonioli et al.*, 2015]. Referring to bioerosion, it is generally assumed that horizontal galleries of coring and boring organisms, frequently submerged by periodic tides, are most active in the midlittoral zone that extends across the tidal range [e.g., *Pirazzoli*, 1986; *Evelpidou et al.*, 2012a]. Thereby, sheltered and vertical exposures are promising locations for the preservation of symmetrical sea-level markers.

*Antonioli et al.* [2015] point out, that salt weathering, wetting and drying cycles, the potential of karst dissolution, and wave action also play important roles in notch formation. The occurrence of a spray zone in more exposed sites introduces a physiochemical erosion component in terms of salt weathering, where the deposition of salt crystals and hydration will modify the notch shape. *Porter et al.* [2010] demonstrated that intertidal wetting and drying and salt weathering is also possible. Dependent on the frequency and duration of tidal immersion and exposure intervals periods for salt crystallization within cracks and fissures are formed supporting this type of haloclastic weathering. Chemical erosion through the dissolution of carbonates is not a common effect of seawater exposure, which is (over-) saturated with $CaCO_3$ [*Kelletat*, 2005b]. The content of calcium carbonate may be lowered only in very localized coastal sections next to springs that show evidence of solution by effluent groundwater [*Evelpidou et al.*, 2012b]. Indeed, nearby freshwater sources support karst dissolution and therefore increase the erosion rate [*Evelpidou et al.*, 2015, 2016]. The vulnerability to different types of physical erosion on coastal cliffs is influenced by the resistance of the rock to wave attack, which is a function of lithology and structural discontinuities, such as cracks, fissures, joints, bedding planes and faults [e.g. *Kershaw & Guo*, 2001; *Trenhaile*, 2014, 2015]. The rock is even more affected when turbulent water contains air that gets compressed when smashed against the rock and causes cavitation pitting [*Antonioli et al.*, 2015]. However, cliff collapses are rare for Mediterranean limestone coastlines [*Trenhaile*, 2016]. Thick-bedded neritic limestones support the overburden and hence the preservation of decimeter-scale deep incisions (Fig. 2). Furthermore, most of these Mesozoic limestones are often not deformed by tectonics; e.g. the massive Parnassos and Gavrovo-Tripolis Units crossing the Corinthian Gulf in central Greece comprise of 1.5-3 km thick neritic mostly undeformed limestones [e.g. *Papanikolaou*, 1984; *Papanikolaou & Royden*, 2007].

As a function of the erosion rate, the period of balanced eustatic sea-level rise and isostatic regional uplift controls how deep an indentation develops. However, eustasy, isostasy, and vertical tectonic movements exhibit considerable spatial and temporal variability throughout the Holocene [*Lambeck et al.*, 2004] (Fig. 1). *Boulton & Stewart* [2015] compared local sea-level curves with associated regional uplift estimates and concluded that the highest elevation tidal notch on uplifting coasts should date to ~6,000 yrs BP. Not until that time did the rate of eustatic sea-level rise decrease to ~1 mm/yr and reach gravitational equilibrium with the continental lithosphere [*Carminanti et al.*, 2003; *Stocchi et al.*, 2005]. In his modelling approach Trenhaile [2016] concludes, that notches develop as long as sea-level change is no greater than 5.6 mm/yr. For the Mediterranean, sea-level rise decreased to this rate ~6,800 years ago. Subsequently, slow relative sea-level changes have caused gradual changes of the erosional base at emerging coastlines.

By contrast, discrete notch levels record abrupt shoreline changes caused by local seismic displacements. In order to preserve the shape and fragile inter-tidal fauna, rapid removal from the tidal zone and lift beyond the reach of waves is needed [*Boulton & Stewart*, 2015].. However, in rifting regions shallow normal faulting events of $M \leq 7$ commonly

produce coseismic uplift limited to a few decimeters along the footwall of the causative fault. Along such faults the uplift/subsidence-ratio is estimated to be ½ to ¼ of net slip per event [e.g. *Stewart & Vita-Finzi*, 1996; *Armijo et al.*, 1996; *McNeill et al.*, 2005; *Papanikolaou et al.*, 2010]. Even in microtidal environments, such as the Mediterranean Sea, rapid displacements due to coseismic uplift most likely do not exceed the tidal range.

Therefore, as a consequence of both, slow and rapid variations in the position of the erosional base, notch shape modification occurs. To distinguish between notch widening and new notch development is challenging (Fig. 3). It has to be expected, that the time period for notch formation might be short and the resulting indentation is only of minor scale, and that massive overprinting and degradation of older features has occurred since ~6,000 years BP.

In order to evaluate stagnation and shifting of the erosional base projected on a present-day cliff face, the long-term geodetic motion should be considered. However, the vertical component of the Mediterranean geodetic field varies dramatically. Continuous GPS stations all over Europe highlight the presence of spatially coherent patterns of uplift and subsidence (Fig. 1). *Serpelloni et al.* [2013] presented up to 14 years of vertical GPS ground motion rates for the Mediterranean region. Their results show that the fastest subsidence of ~-3 mm/yr is located in southern Spain, while general uplift (~2 mm/yr) is obtained for the Alps. Furthermore, the dataset indicates landmass uplift of ~1 mm/yr towards the eastern part of the Mediterranean Basin, such as for the island of Crete and the Cyclades. However, the network density here is significantly lower than in central Europe, thus the vertical deformation is less well constrained for the eastern Mediterranean. In addition, the precision of vertical positions determined by most GPS station is ~1 mm/yr [*Sepelloni et al.*, 2013; *Faccenna et al.*, 2014] and observation periods are small in comparison to geological timescales [*Papanikolaou et al.*, 2005].

Long-term Quaternary activity is generally reflected in coastal geomorphology, including uplifted Pleistocene marine terraces and notches of Holocene age in steep calcareous cliffs. Benefits of dating such features are that they represent approximations of cumulative rates over multiple seismic cycles [*McNeill & Collier*, 2004]. Nevertheless, variations in vertical movements across the Mediterranean region are also presented by several studies (Fig. 1). For the western Mediterranean only very minor uplift rates are obtained [e.g. *Zazo et al.*, 1999, 2003]. In the central region, predominantly concentrated at the coastlines of Sicily and southern Italy, several studies have been undertaken calculating uplift rates ranging from 1.0 – 2.4 mm/yr [e.g. *Westaway*, 1993; *Stewart et al.*, 1997; *Antonioli et al.*, 2006]. The rapidly extending Corinthian Gulf produces Holocene uplift rates of 0.3 mm/yr in the eastern parts up to 1.5 mm/yr in the most western parts [e.g. *Stewart & Vita-Finzi*, 1996; *Leeder et al.*, 2003; *Cooper et al.*, 2007]. While close to the Hellenic Subduction Zone (HSZ) *Roberts et al.* [2013] calculated an average uplift rate of 1.0-1.2 mm/yr derived from marine terraces at the island of Crete. For the southern margin of the central Anatolian Plateau (CAP) estimates for Holocene uplift range from 0.6 to 0.7 mm/yr [*Schildgen et al.*, 2012]. By contrast, the Levantine coastline is assumed to be tectonically stable for the past 10 ka [e.g. *Sivan et al.*, 2001, 2004; *Goodman-Tchernov & Katz*, 2015].

## 3 Dynamic notch formation

In the first instance, the rate of relative sea-level change determines whether a tidal notch will develop or not. For the Mediterranean, estimates of limestone erosion rates range from 0.2-1.0 mm/yr [*Pirazzoli & Evelpidou*, 2013; *Evelpidou & Pirazzoli*, 2016]. Thus, balanced conditions between eustasy and isostasy have to persist for about 200 years to

develop a significant 20 cm deep notch. The notch height would approximately equal the tidal range for which estimates range from 0.3 – 0.4 m for the majority of the Mediterranean [*Evelpidou et al.*, 2012b; *Evelpidou & Pirazzoli*, 2016], although exceptional tides of up to 1.8 m may occur in the northern Adriatic [*Trenhaile*, 2016]. Shape modification is given by exposure, and/or organic accretions [*Pirazzoli*, 1986; *Antonioli et al.*, 2015]. Increasing exposure yields an upwards shifted roof while the base remains at low tide level. Thus, the height of a notch is primarily controlled by exposure to wave action. Biological accretions are located at the base of a notch. If present the lower part of the notch is no longer a mirrored copy of the upper part but reduced in size. However, a simplified description is supported by sheltered conditions and the absence of biological accretions. Then, the coefficients of a quadric polynomial can cover the requirements to describe such symmetrical shapes (Fig. 4). As in a conceptual static model, notch depth is specified by erosion rate [mm/yr] x time [yr] of a constant erosional base.

The dynamic model (considering actual relative sea-level change; Fig. 3) calculates the parabolic erosion for every year considering both rapid and slow relative sea-level changes and computes the cumulative sum of erosional impacts. Using a local sea-level curve and information regarding ongoing isostatic and dated coseismic uplift as inputs to control the migration of the erosional base enables us to describe the vertical cliff morphology at a given moment.

## 4 Methodology

The modelling algorithm developed here incorporates eustatic and isostatic balances, erosion rates, cliff steepness, and coseismic uplift. Therefore, the input parameters that have to be specified for the model are: I) the tidal range [m]; II) the erosion rate [m/yr]; III) a long-term coastal uplift rate [mm/yr] and eustatic information (e.g. *Lambeck & Purcell*, 2005), and IV) the average steepness of the cliff in degrees. Values of coseismic uplifts [m] from one or more events are optional, but have to be linked to a number of years BP if given.

The initial conditions in the model are characterized by an infinite cliff. The influences of the cliff slope are widely discussed in *Pirazzoli* [1986, Fig. 3] yielding in asymmetrical notch shapes when different from a straight 90-degree [see also *Trenhaile, 2016*]. In order to run predictions from the most favorable conditions [*Pirazzoli*, 1986] the initial setting corresponds to situations where the cliff is vertical.

Following the static model idea, notch development occurs at sea-level and does not change through time. The depth *d(z)* of the notch at different stages is expressed as a quadric polynomial as follows:

$$d(z) = az^2 + bz + ER * dt \qquad \text{[eq. 1]}$$

where the coefficients *a*, *b*, and *ER* define the co-domain and shape of the graph in accordance to the erosional base. The erosion rate *ER* provokes a translation in y-direction and represents the eroded depth after one year (*dt*) at mean sea-level. The parameter *b* is the gradient at the y-axis. However, when mean sea-level is set to zero the inflection point is located at the y-axis. Hence, the gradient *b* is zero. The curvature at the inflection point is defined by *a*. Thereby, the roots at floor and roof, respectively, act as targets the graph has to pass. Since these are given by the extents of the tidal range, they can be utilized to transcribe *a* as a function of the erosion rate as follows:

$$a = \frac{f(z)}{(eb - z_{s1}) * (eb - z_{s2})} \qquad \text{[eq. 2]}$$

Here, *f(z)* is the determined depth in succession of one year of penetrating erosion. *eb* depicts mean sea-level and is set to zero. The roots $z_{s1}$ and $z_{s2}$ represent the floor and the roof of the notch and hence obtain values of half the tidal range with different sign.

In order to consider the change of the erosional base through the Holocene, the difference between a given sea-level curve and applied coastal uplift is included. When correcting a sea-level curve for the isostatic trend, the time of notch formation is indicated for periods where the gradient is ~0 (Fig. 5a). Afterwards, the Cartesian grid is translated for every year, so that the origin always equals the erosional base. Thereby, the grid translation circumvents complex recalculations of *a*. Indeed, the result is an examination per year. Therefore, a matrix (size: elevation, years BP) is generated incorporating the cumulative sums of each simulated profile. Consequently, the last array of the matrix represents the modelled notch sequence covering the entire vertical extent of affected parts during the simulation. Furthermore, by calculating the erosional base it is also demonstrated that the erosive zone does not project below -3 m (Fig. 6). We assume that this is shallow enough to exclude larger scale morphologies such as continuously submerged shore platforms from the model.

The purpose of this paper is to simulate vertical coastal cliff evolution during the late Holocene visualizing the interplay between slow and rapid regional-scale contributors to changes in erosional efficacy. Therefore, the model is simplified, refraining notch shape influencing parameters such as wetting and drying cycles and salt weathering, predicting vertical cliff profiles only for sites with high potentials of tidal notch development and preservation. Following the suggestions from *Pirazzoli* [1986], cliffs sheltered from wave action located in a microtidal environment pose ideal sites for tidal notch development with a minimum of shape modification and best preconditions for tidal notch preservation. For the central and eastern Mediterranean low-moderate wave energy potentials with mean values around 6-7 kW/m are presented in *Besio et al.* [2016]. Altimeter significant wave height measurements suggest mean values of ~1 m for the entire Mediterranean Basin [*Queffeulou & Bentamy*, 2007]. In calm and semi-enclosed sub-basins within the Mediterranean such as the Tyrrhenian coast, the northern Adriatic, the Ionian Aegean Sea, and the Levantine coast, wave heights are up to 0.6 m with wave periods of around 1-5 s [e.g. *Ayat*, 2013; *Liberti et al.*, 2013]. Furthermore, we are referring to tidal notches which do not have to be confused with other marine notches formed by sediment abrasion. Closely located sediment sources such as beaches and strong currents may support the development of such abrasional notches, which do not necessarily correspond to the tidal range. Moreover the amount of bioerosion is minimized in such grinding environments [*Kelletat*, 2005b]. An important condition for tidal notch preservation is the bedrock lithology. Databases on tidal notches in the Mediterranean [e.g. *Boulton & Stewart*, 2015] show that they mostly occur in neritic thick-bedded or even massive limestones. Besides that cliff collapse is uncommon in the Mediterranean [*Trenhaile*, 2016] due to lithological conditions (see Fig. 2), considering cliff failure is irrelevant for decoding the cliff evolution of an actual cliff where preserved paleostrandlines can be observed.

## 5 Results

In order to demonstrate how sensitive the algorithm is for differing input parameters and how diverse notch development occurs through time we applied local conditions of eight different regions across the Mediterranean to the algorithm (Tab. 1). Furthermore, coseismic activity is included in the model for two specific sites (Fig. 1b, Tab. 2).

### 5.1 Uplifting coastal regions: Western/Eastern Gulf of Corinth and eastern Sicily and Calabria

The Mid-Holocene sea-level curve for the Peloponnese coast (Greece) from *Lambeck & Purcell* [2005] shows a monotonically increasing sea-level and does not contain characteristics such as a mid-Holocene highstand or punctuated parts (Fig. 6a,b). At ~7,000 yr BP the rate of sea-level change decreases considerably and potentially forms conditions for relative sea-level stagnation at ~6,000 yrs BP, when applying an average coastal uplift of 1.2 mm/yr [*De Martini et al.*, 2004]. After correcting the curve for the uplift trend, the resulting gradient allows the timing of notch development to be described (see Figs. 3, 5a). The result of 7,000 years of a vertically shifting erosional base is shown in figure 7. Almost 6.8 kyr BP notch formation begins and corresponds to a 15 cm deep notch ~1.4 m above present-day sea-level. A minor variation and sea-level rise ~6.1 kyr BP yields an upward shift of the erosional base. Not until 5.9 kyr BP is the next equilibrium is reached. During the period in between an upward grazing occurs which indicates that the rate of sea-level change is still slow enough to significantly erode the limestone. From 5.9 – 2.6 kyr BP, a period of almost no sea-level change occurs at a corresponding height of ~2 m resulting in an indentation of almost 1.5 m depth and ~0.4 m height, at an erosion rate of 0.5 mm/yr. The subsequent gradual and slow lowering of the erosional base until present-day sea-level produces and overprints the first stage of notch formation. From a present-day view a notch appears at ~1.5 m which is actually the result of two erosional phases 6.5 kyr and 2.5 kyr BP, respectively. It should be noted that the first period yields in a 15 cm deep notch that gets heavily overprinted by the second phase. To conclude cliff morphology evolution for the western Gulf of Corinth, an entire sequence of three notches at ~2 m, ~1.5 m and present-day sea-level can develop without any rapid vertical motion of the strandline.

The same sea-level curve forms the input for the eastern Gulf of Corinth simulation. The highest extensional rates of up to 15 mm/yr are estimated for the western part of the Gulf. Long-term vertical movements towards the Alkyonides Gulf are lower; where, a net uplift rate of 0.7 mm/yr is applied following estimates of *Stewart & Vita-Finzi* [1996] [see also *Roberts et al.*, 2009]. The resultant modelled cliff section is markedly different to that predicted for the western Gulf of Corinth. The trend corrected sea-level curve does not reach its stagnation phase, where the gradient is almost zero, until ~3 kyr BP (Fig. 6b). However, at ~6.8 kyr BP the rate of change is small enough so that the erosive potential penetrates almost the same area over a considerable time period at a corresponding height of -1.9 m. Gradual vertical shifts during the period between ~6.2 and 6 kyr BP graze the rock no deeper than 0.1 m but across ~ 1 m in height. Hereafter, the rate of sea-level change decreases again increasing the penetration time and supporting the development notch of a small notch. At ~ 5 kyr BP a third decrease in sea-level gradient occurs, but which is still faster than the 0.7 mm/yr uplift. Corresponding to todays' sea-level the erosional zone is located -0.5 m during that stage (Fig. 7b) and shifts to the present datum ~3.8 kyr BP. Subsequently, a fourth stage of a lowered sea-level change gradient causes an increasing indentation at a corresponding height of ~0.2 m. However, very minor gradual changes widen the developing notch. The stagnation is then reached ~3 kyr BP. This phase lasts for ~2,000 years ending up in a final stage of gentle lowering the erosional base. The last 1,000 years are dominated by forming the present-day tidal notch of > 1 m depth that overwrites pre-existing erosive structures.

The sea-level curve for the north-western part of the Ionian Sea also has two main periods of rising sea-level. The transition between both is not as clear as for the Gulf of Corinth but ~6.5 kyr BP sea-level rise stopped outpacing an uplift of ~1.0 mm/yr [*Westaway*, 1993; *Tortorici et al.*, 1995; *Stewart et al.*, 1997; *Ferranti et al.*, 2007]. When the sea-level curve is corrected for this uplift trend, the erosional base has two minor rising steps at ~5 kyr

and 3.5 kyr BP, respectively (Fig. 6c). The highest erosional level of ~2 m dates to ~3 kyr BP before it decreases to present-day sea-level. A more detailed view is given by corresponding time slices in figure 8. Incision into the cliff began 6.4 kyr BP when the rate of sea-level rise decreased significantly. However, not until 5.5 kyr BP is the gradient low enough to form a distinct indentation at a corresponding height of ~0.4 m. The penetration period lasts ~600 years when a gradual upward shift of the erosive base for ~0.5 m occurs, resulting in a widening of the indentation. Around 4.8 kyr BP the erosion occurs at a corresponding height of ~0.9 m and forms a notch of ~0.5 m depth at 0.8 m asl. Subsequently, another upward shift ~3.3 kyr BP causes a third distinct indentation at ~1.2 m asl. An equilibrium state for > 1,000 years yields not only in a resulting notch depth of up to 0.8 m but also overwrites the roof topography of the underlying notch. During the period between 1.8 kyr BP and 1 kyr BP successive lowering of the erosional base causes a downward widening of the latest indentation and erosion of former notch topographies. The subsequent stage is dominated by grazing the cliff downwards and again of overprinting structures that formed ~4,500 years earlier. Today, the erosive sequence shows three to four notches (+1.2, +1.0, +0.4, and currently forming) which match up with elongated periods of relative sea-level stagnation but their depths are heavily altered during grazing phases.

5.2 Moderately uplifting coastal regions: southern Turkey and eastern Aegean Sea

For the southern margin of the central Anatolian Plateau (CAP, southern Turkey) uplift at 0.7 mm/yr was estimated by *Schildgen et al.* [2012]. This rate slightly outpaces the local sea-level curve within the period of the last 6,000 years. However, the rising rate of sea-level change is characterized by very minor variations so that the corresponding erosional base evenly decreases from ~1.4 m to the present datum (Figs. 6e and 9a). The development of the cliff morphology is characterized by distinct notch formation for about 1,500 years from 6-4.5 kyr BP, subsequent lowering of the erosional base resulting in extensive downward grazing, and again focused notch formation at ~0.7 m from 4-2.5 kyr BP, removing the floor of the earlier feature. A subsequent minor shift of ~0.1 m causes a third indentation just below the last. The present-day notch is the result of gradual down-shifting the erosional base.

By contrast, a distinct knickpoint forms at ~6 kyr BP along the coast of Samos Island (Fig. 6h) where the net uplift is estimated at 0.6 mm/yr [*Stiros et al.*, 2000], which is comparatively low but matches the overall rate of sea-level rise for the last 6,000 years. Consequently, notch development occurs along a very narrow horizon for the Mid-Holocene period (Fig. 9b). Ongoing erosive penetration against the cliff appears at ~5.8 kyr BP resulting in a notch of ~0.7 m depth at a corresponding height of 0.7 m. A minor shift of ~0.2 m towards todays' datum causes distinct notch formation from 3.5-1.5 kyr BP. The present day tidal notch forms during the last 1,000 years, resulting in a single composite notch.

5.3 Tectonically stable regions: Tuscan coast and Carmel coast

A short period (7.5-7 kyr BP) of lower rates of sea-level rise followed by again steep rising before sea-level change adjusts at a moderate slope ~6.5 kyr BP is the most characteristic part of the Tuscan coast Mid-Holocene sea-level curve (Fig. 6d). *Lambeck et al.* [2004] stated that the shorelines along the northern and central Thyrrenian coasts are largely free from vertical tectonic movements and uplift is only at 0.2 mm/yr in the Holocene interval. Therefore, trend correction to estimate the erosional base has only a minor influence on rates of sea-level change. Potentially, tidal notch development initiates 2.9 kyr BP without further noteworthy vertical changes. From the time slices (Fig. 10) it is obvious that considerable grazing of the cliff began ~6.7 kyr BP. Approximately 1,000 years later the rate

of sea level change lowers again and causes deeper grazing up to ~0.1 m. However, ~2.9 kyr BP a distinct notch begins to form, at around -0.8 m. Subsequent lowering the rate sea-level rise causes enhanced penetration per level while still distinct widening can be observed. A distinct notch is finally formed at ~0.7 kyr BP with the inflection point just below present-day sea-level (Fig. 10).

The sea-level at Carmel Coast (Israel) has risen by not more than ~4 m since ~6.8 kyr BP; with only ~0.5 m increase during the last 2,800 years. This means that from 6.8-2.8 kyr BP sea-level rises in average at ~0.9 mm/yr, and afterwards at ~0.2 mm/yr. The latter rate coincides with uplift rates estimates by *Sivan et al.* [2001] (Fig. 6f), which is why notch formation is expected to occur during the latest times of the Holocene; and furthermore not higher than at present datum. However, the results in figure 10 show that the potential of considerable erosion is already given 5.8 kyr BP. The erosional base evenly rises until ~3.9 kyr BP and causes a 1 m wide band along the vertical cliff with an average period of water contact of ~300 years; the resulting depth is ~0.15 m. A subsequent period of ~1,100 years prolongates the contact time to ~400 years due to a lowered rate of sea-level rise. At an erosion rate of 0.5 mm/yr the cliff gets deepened by 0.2 m during that period (Fig. 10b). Since the given tidal range of 0.3 m already extends to the corresponding datum at that time, the floor of the most recent notch develops. A complete overlap of both rates, sea-level rise and net uplift, occurs for the last 900 years resulting in a notch of >1 m depth at present-day sea-level.

It is obvious that both regions experience similar evolution of tidal notch development. For both regions the same net uplift values are applied. The differently shaped sea-level curves determine the calculated depth and significance of modelled notches. However, overall evolution and resulting cliff morphology bear resemblance at both parts of the Mediterranean.

### 5.4 Subsiding coasts: NE Adriatic Sea

Coastal subsidence [-0.35 mm/yr; *Lambeck et al.*, 2004] causes steeper gradients within the evolution of erosional levels than coastal uplift (Fig. 6g). The trend corrected sea-level curve for the NE Adriatic has average rates of ~1.2 mm/yr from 6-2.7 kyr BP and ~0.4 mm/yr since 2.7 kyr. Therefore, indentations are expected to be not as deep as in uplifting regions. Modelled time slices in figure 11 reveal that erosion begins ~6 kyr BP carving the cliff down by ~0.1 m. This means, already by that time the erosional zone affects the same cliff section for ~200 years at a modelled erosion rate of 0.5 mm/yr. Except for a few minor vertical undulations the resulting cliff is carved by the same rate for the subsequent 3,300 years. At approximately 2.7 kyr BP the lowered gradient of erosional base migration causes deeper incision at >-1 m asl on the modern cliff (Fig. 11). The erosion rate exceeds the absolute vertical motion value which results in predominant notching rather than widening of the indentation. However, the recently developing notch at ~-0.2 m asl is 0.3 m deep and is the result of a gradual uplift shift of the erosive tidal zone.

### 5.5 Introducing cliff slope and coseismic activity to the model

*Pirazzoli* [1986] already pointed out the influence of sloping cliff faces. In particular, cliffs dipping gentler than 90° require more time to develop distinct notch morphologies, and the resulting notch shape will be asymmetrical with short roofs and long floors. However, this is the result of cumulative erosion over several years. The erosional potential remains normally distributed within the tidal range, which is why only the dip of the cliff face has to be adjusted in the model input. Here, a moderate-high angle cliff slope of 80° is chosen causing asymmetrical notch shapes while preserving the ability to form distinct features.

A famous cliff face exhibiting tidal notch morphologies that are repeatedly associated with coseismic events is located at the north-western tip of Perachora Peninsula in the Alkyonides Gulf [e.g. *Kershaw & Guo*, 2001; *Pirazzoli & Evelpidou*, 2013]. *Pirazzoli et al.* [1994] identified four shorelines each offset by ~0.8±0.3 m with estimated recurrence intervals of 1,600 years from dating organic material of three notches at Heraion (tab. 2). The strandline that was not dated (+1.7 m asl.) by the authors is here calculated in accordance to the estimated recurrence interval and average displacement.

Introducing coseismic uplift events creates a stepwise modification to the emerging coast function in our model (Fig. 12a). Dependent on the rate of relative sea-level change the adjustments to the function representing coastal movements cause a prolongation of notch formation or result in the development of a new notch generation. Considerable erosion begins ~6.6 kyr BP and thus forms no difference to the model without coseismic uplifting events. However, a much higher position (~+0.6 m) on the modern cliff face than without a correction for relative vertical land movements (~-2.4 m; see Fig. 7b) is obvious. A significant shift occurs until ~5 kyr BP ending up in notch formation at ~+2.5 m (asl.) prior to coseismic event 1. The first event lowers the erosional base by 0.6 m. As a consequence the former strandline is lifted above the tidal range and a new notch generation develops at ~+2.2 m (asl). At that time (~4.4 – 2.4 kyr BP) the rate of sea-level rise is still significantly different from the applied uplift rate causing upward carving and erosion of pre-existing erosional features. Prior to event 2 the erosional base is located at ~+2.8 m (asl.) forming a second notch generation during relative stagnation of ~300 years. The accompanying 0.9 m coseismic uplift of event 2 throws the erosive zone back to a corresponding level at ~+2.0 m. As the modelled scenario without coseismic uplift events already showed (see Fig. 7b) the last ~2,000 years are dominated by stagnation of the erosional base. Thus, in periods between events 2 and 3, and between events 3 and 4 distinct notches form at ~+2.0 m and ~+1.3 m (asl). The sloping cliff morphology causes an asymmetrical appearance of both notch generations as predicted by *Pirazzoli* [1986]. Subsequently, event 4 displaces the pre-existing prominent strandline and results in the development of a new notch generation at modern sea-level. The projection of the erosional base on the modern cliff face shows slight shifting prior to ~ 2.5 kyr BP. As a result, vertical carving instead of horizontal deepening is the dominant erosive factor. Excluding the recently developing tidal notch the cliff face exhibits three to four distinct indentations whose individual position on a modern cliff are further associated with coseismic events.

A second scenario including coseismic uplift events is modelled for the western Gulf of Corinth. Estimates on coseismic footwall uplift values per event and dated shorelines from *Stewart & Vita-Finzi* [1996] serve as input parameter additional to those already introduced in section 5.1. The authors dated two raised shorelines (1.8 m and 3.7 m asl.) along the Eliki Fault to 1680 ± 130 yr BP for the lower strandline, and 2290 ± 115 yr BP and 2600 ± 265 yr BP for the upper notch. Furthermore, they found no expression which can be attributed to a surface rupturing event that happened 1861 AD. However, from these dates an earthquake recurrence interval of ~700 years is assumed here. Earthquake events of M6.0-7.0 as found from normal faulting events elsewhere tend to produce coseismic footwall uplifts of 0.2-0.3 m [e.g. *Jackson et al.*, 1982; *Papanikolaou et al.*, 2010]. Therefore, the scenario includes 11 earthquakes accompanied by normal distributed coseismic uplifts ranging from 0.2-0.3 m within a period of ~8,000 years (tab. 2). Events 1 and 2 produced surface displacements during periods of unstable sea-level conditions. Therefore, no offset erosional expressions result from these two events. The first notch begins to form ~6.7 kyr BP at ~+3.6 m but widens up to a level of ~+4.1 m because of minor sea-level changes outpacing the coastal uplift. Event 3 lowers the erosional base to a corresponding height of ~3.9 m. The subsequent

700 year period is dominated by stagnation of the relative erosional base forming a distinct notch of ~0.3 m depth (Fig. 13b IV). The ensuing period of ~1,400 years contains two events (4 and 5) that stepwise lower the relative erosional base which stays at a gradient of almost zero apart from that. The resulting notches (V and VI) comprise erosional contributions from 3,000 years before. A distinct notch (VII) forms from ~3.8-3.0 kyr BP without noteworthy vertical shifting. During the period between event 7 and 8 notch VIII develops at ~+2.8 m but gets widened due to a small component of gradual lowering the relative erosional base. The same process happens to notch IX that develops at ~2.0 kyr BP. Even more obvious is the widening effect for the last two notches (X and XI), which are still separated from each other due to the successive uplifts from events 9 and 10. However, a sea-level rise slower than modelled uplift causes a gradual lowering of the relative erosional base in the latest Holocene period. The predicted modern cliff morphology shows nine different historical sea-levels ranging from ~+0.7 m to +4.0 m. While uppermost notch generations (III - VI) appear stacked and concentrated, younger notch generations (IX - XI) are more spread along the vertical cliff. Presumably, the uppermost notch generations (III-VI) would not be differentiable in the field since their vertical spread is only 0.5 m and thus just exceeds the applied tidal range.

## 6 Discussion

The focus of this study has been to visualize tidal notch formation during the late Holocene, incorporating sea-level change, coastal uplift/subsidence, erosion rates, coseismic activity, and cliff steepness. We have been able to show how coastal cliff morphologies develop within a migrating tidal range [see also *Pirazzoli*, 1986; *Evelpidou et al.*, 2011a,b; *Trenhaile*, 2016] using actual late-Holocene sea-level curves for the Mediterranean. The tidal range shifts along a vertical cliff due to gradual relative sea-level changes optionally accompanied by coastal tectonic activity. In the following discussion, the contributions of slow and rapid vertical shifts of the erosional base are discussed with regards to the applied modelling parameters.

### 6.1 Modelling parameters and inputs

The modelling algorithm we present here deals with ideal conditions. Therefore, the results do not represent actual and naturally existing cliff faces.

Firstly, these ideal conditions incorporate a perfectly sheltered site, where tidal range is low and constant [*Pirazzol*i, 1986]. Assuming the absence of spray enables us to ignore notch roof modification by haloclastic processes above the high tide level. In addition, carbonate lithologies sheltered from strong wave action enable grazing or coring organisms to settle and contribute to the erosion in vegetational bands within the midlittoral zone [Torunski, 1979]. Moreover, *Pirazzoli* [1986] points out that only in sheltered sites does the midlittoral zone equal the tidal range. Since the model calculates erosive effects only for the applied tidal range of 0.3 m [*Evelpidou et al.*, 2012b; *Evelpidou & Pirazzoli*, 2016], predicted profiles correspond to natural sites without strong wave action. If a different tidal range is used, then the affected parts of the cliff vary accordingly. Hence, a smaller tidal range yields narrower indentations whereas a wider tidal range increases width of a tidal notch [see also *Trenhaile*, 2014]. When the erosional base varies through time narrow notches appear to have greater separation than wider features.

Secondly, the algorithm was designed to model tidal notches formed within the tidal range without significant contributions by wave quarrying, sediment abrasion or chemical weathering. Mechanical wave erosion is of a second order when unbroken waves are reflected from steep cliffs and when a source for abrasive material is absent. Moreover, wave quarrying is most common in storm wave regions and where coastal cliffs are comprised of rocks with structural discontinuities [*Trenhaile*, 2015]. The majority of carbonate coastlines throughout the Mediterranean do not have plunging cliffs and/or are located next to beaches, or are fronted by wave breaking foreshores. However, steep cliff faces of massive limestones located far from abrasion material such as sands and pebbles exist. Indeed, carbonate cliffs tend to develop karst formations which may be accompanied by freshwater exchange. If so, the sea-water is locally diluted and thus chemical dissolution of calcium carbonate contributes little to the overall erosion rate. Moreover, the solubility of calcium carbonate is higher at low temperatures. This leads to the assumption that during the glacial period lower water temperatures in general and higher precipitation resulted in higher amounts of limestone dissolution. However, *Evelpidou et al.* [2011b] suggest using the term ‘visor’ for notch profiles where the base is missing due to chemical dissolution. For such localized phenomena notch developing effective erosion is not limited to the tidal range and hence those morphologies are not suitable sea-level markers. Herein, model predictions aim to illustrate the evolution of paleostrandline sequences as they are commonly used to infer coastal coseismic activity [e.g. *Pirazzoli et al.*, 1982, 1989, 1991, 1994; *Stewart & Vita-Finzi*, 1996; *Kershaw & Guo*, 2001]. Furthermore, late Holocene tidal notches develop in the hot

and semiarid environment of the Mediterranean. This circumstance decreases the ability of limestone dissolution, in general.

Thirdly, vertical lithological inhomogeneities are not considered. Varying bedrock consistency and accompanying erosion rates are not modelled. Consequently, the profiles represent homogeneous limestone cliff morphologies resulting from even erosion at 0.5 mm/yr [e.g. *Evelpidou et al.*, 2012b; *Furlani & Cucchi*, 2013, *Pirazzoli & Evelpidou*, 2013]. Dating tidal notches and deriving erosion rates is a challenging task since radiocarbon-bearing dating material is of very sensitive organisms that can easily be eroded by various agents after their displacement [e.g. *Evelpidou & Pirazzoli*, 2016]. However, some efforts have been undertaken to derive estimates for erosion rates across the Mediterranean. The applied erosion rate is in good correlation with recently derived estimates from a well-dated fossil tidal notch in Greece (0.64 mm/yr) [*Evelpidou & Pirazzoli*, 2016] and from micro-erosion meter measurements in the northern Adriatic (0.31 mm/yr) [*Furlani & Cucchi*, 2013]. In general, it should be noted that varying the applied erosion rate in different model runs modifies the predicted indentation depth but not its position [see also *Trenhaile*, 2014].

Fourthly, modelled notches are not constructed to collapse. Overburden that cannot be supported by the lithology results in cliff collapse, which is basically controlled by the depth of a notch. *Trenhaile* [2014] includes the ability of cliff collapse in his modeling approach and concludes that failure is mainly dependent on the maximum notch depth. For collapse scenarios the author used maximum notch depths of 2 m. However, the notch profiles predicted herein do not exceed 1.5 m in depth (see Fig. 7a). Moreover, if cliff collapse occurs environmental conditions change likely resulting in significantly different wave action and constitute a possible sediment origin [*Trenhaile*, 2015]. This would clearly contradict other model assumptions at a certain point.

Fifthly, horizontal differences are not displayed by a two dimensional notch profile. Fault movement leading to differential uplift, local variations of wave and surf regimes, and horizontal bedrock heterogeneity are reasons for differing notch profiles on a local scale [e.g. Kershaw & Guo, 2001].

The five listed caveats imply significant simplifications to the model. Each of above mentioned points has considerable influence on the shape of a notch profile. Furthermore, the combination of all of them is considered to modify a tidal notch for each investigated region individually. However, considering such assumptions enables the development of a mathematical model of a symmetrically effecting erosion potential within the tidal range per year. Then, cumulative erosion depicts the base for the static notch developing model that only distinguishes between continuous erosion per level or not.

Predicting actual scenarios using local sea-level curves and regional landmass movements is a novelty to the assessment of tidal notches as earthquake geological effects. Conceptual models [e.g. *Pirazzoli*, 1986; *Evelpidou et al.*, 2011a,b] indicate shape modification by sea-level change and even already distinguish slow and rapid changes of the erosional base. *Trenhaile* [2016] modelled notch formation considering linear and sudden sea-level changes as well. In contrast to the model presented in here, the author also considers changing erosional efficacy, cliff collapse [see also *Trenhaile*, 2014], and varying rock resistance. However, by simplifying the model assumptions and orienting to specific regions we were able to achieve similar conclusions regarding the influence of local- and regional-scale factors, and to confirm that. similar profiles can be produced by different combinations of incorporating factors [see *Trenhaile*, 2016]. One difference between Trenhailes's and our models is the applied distribution of the erosional potential. Where *Trenhaile* [2016] uses a linear function we consider a distribution following a quadric polynomial based on repeated

immersion of cliff parts due to tides following a sine function in a long-term average (Fig. 4). Erosion rates measured at different heights (vertical resolution is 0.25 m) over a 3-year period on a limestone slab in the northern Adriatic indicate that the mean downwearing rate follows a symmetrical shape [*Furlani & Cucchi*, 2013]. Long-term measurements will show what is the best fit function describing the erosional potential distribution. However, since both models yield similar results the fitting appears to be of a second order. As a major difference between both models *Trenhaile* [2016] constructed a more theoretical approach, while we clearly orient at region-specific conditions. Hence, our model provides the opportunity to compare natural occurrences of tidal notch sequences with derived scenario interpretations. Existing investigations and interpretations on coseismic tectonic history might have to be reassessed due to so far unknown consequences concerning submerged notches and/or timing and magnitude of coastal coseismic activity.

Therefore, the most dynamic component in the model is the applied sea-level curve. The shape, rates, punctual characteristics, and the overall richness of details of a sea-level curve form fundamental input for the dynamic model (Figs. 6 and 10). Commonly, a variety of sea-level indicators are used to reconstruct sea-level history. Typically, these indicators are of biological, sedimentological, erosional, and archaeological remnants [*Lambeck et al.*, 2004; *Kelletat*, 2005a]. However, the spatial distribution across the Mediterranean, concentration of certain markers in some places, and differential tectonic activity cause gaps in the availability of local sea-level curves (e.g., Spain, North Africa) [*Pirazzoli*, 1991] and vary the quality. By contrast, many sea-level curves have been published for shores at southern France, the Aegean, the Levant, and the Adriatic in the past decades. All histories applied here have a significantly changing rate of sea-level rise plotted in the period between 7-6 kyr BP. A global meltwater pulse caused rapidly changing sea-levels (10-20 mm/yr) until 7 kyr BP (Fig. 5a), before slow-moderate (0.2-2 mm/yr) rise adjusts in the Mid-Holocene. *Lambeck et al.* [2014] point out that in the past 6.7 kyr BP only 4 m of global sea-level rise took place, which equals an average rate of ~0.6 mm/yr. Moreover, the authors predict actually two stages of sea level rise, the first going from 6.7-4.2 kyr BP, and the second covering the last Holocene period. Following their estimates, 75 % of Mid-Holocene sea-level rise took place during the first stage (1.2 mm/yr). Sea-level changing at ~0.2 mm/yr during the second stage is broadly consistent with other studies [e.g. *Pirazzoli*, 1991]. For the Mediterranean Sea a third trend of 1.7 mm/yr covering the past century is predicted by *Wöppelmann & Marcos* [2012]. However, the last is not considered in this study since the applied erosion rate of 0.5 mm/yr produces indentation of 5 cm only in 100 years of relative stand-still. Furthermore, this high-rate change still does not submerge the cliff from the tidal range of 0.3-0.4 m [*Lambeck et al.*, 2004; *Evelpidou et al.*, 2012b; *Antonioli et al.*, 2015] within this short period. The local sea-level curves applied to test the algorithm are consistent with overall characteristics described above. However, the relative sea-level at the knick-point around ~6.5 kyr BP varies as well as the timing for the second rate lowering period. While the relative sea-level was ~6-7 m below present datum (Fig. 6a-d) in the central Mediterranean since the Mid-Holocene, a ~3-4 m rise occurred in the eastern parts of the basin (Fig. 6e,f,h). The second, more minor change generally appears between 3-2 kyr BP and thus later as predicted from the global sea-level curve [*Lambeck et al.*, 2014]. Furthermore, in the central basin this change tends to occur at ~3.0-2.5 kyr BP while the eastern Sea reaches this point ~500 years later [e.g. *Sivan et al.*, 2001].

### 6.2 Solving the issue with submerged notches

In regions of significant tectonic activity reconstructing the sea-level history is problematic since most sea-level indicators refer to some specific part of the tidal range and

their displacement by fault activity requires accurate adjustments to resultant vertical motion. *Roberts et al.* [2009] demonstrated the variability in uplift even over short distances along fault strike. Yet tectonic activity is essential for estimates of long-term landmass uplift/subsidence. Hence, for regions such as the seismically high-active Gulf of Corinth it is unlikely that representative estimates for both, sea-level history and paleo-tectonic rates, will be found. In such cases assumptions and spatial generalizations have to be made; for instance, the sea-level curve for the shore of Peloponnese is representative at least for the western part of the Corinthian Gulf.

Interestingly, *Boulton & Stewart* [2015] hypothesized that in order to initiate notch formation uplift rates needed to equal rates of sea-level rise. This statement presumes that subsiding coasts will not experience a relative stagnation under conditions of steadily rising sea-levels and that subsiding coasts are not suitable for tidal notch development without more complex tectonic movements involved during the late Holocene.

The difference between relative sea-level and corresponding landmass position forms the relative erosional base projected on a modern cliff face. Different uplift rates applied to the same sea-level curve have a huge impact on the shape of erosional base evolution (Fig. 6a,b). As a result, tidal notches form at different periods and appear on different corresponding levels (Fig. 7 & 14a). Furthermore, a combination of low coastal uplift rates (< 1 mm/yr) and significant sea-level change since the Mid-Holocene yields tidal notches to appear below present-day sea-level. Coasts that are considered to provide stable conditions potentially exhibit submarine notches (Fig. 10). Here, the model is confirmed by observations made at the southern Levantine coast by *Goodman-Tchernov & Katz* [2015]. The authors concluded sea-level history provides a period of relative stagnation, followed by drowning. At a coast that is generally considered to be not tectonically affected, only eustatic characteristics provide potential for notch development.

The results modelled from subsiding coastal conditions show that relative stagnation does not mean sea-level rise and vertical landmass motion have to occur in unison. In detail, modelled cliffs get significantly carved when the erosional base shifts at <1.1 mm/yr using an overall erosion rate of 0.5 mm/yr [see also *Trenhaile*, 2016]. Moreover, horizontal deepening dominates vertical carving when the difference between vertical land motion and sea-level rise is < 0.5 mm/yr. This implies, a notch in a limestone cliff (erosion rate: 0.5 mm/yr) that develops while sea-level rise or landmass motion dominates by 0.5 mm/yr for about 200 years is ~0.1 m deep and ~0.4 m high (including 0.3 m tidal range). When introducing the effect of varying tides, spray, and weathering the interpretation of such an expression would most likely conclude a "relative stagnation" to form it. Even the occurrence of a notch located on a subsiding coast becomes plausible if vertical relative land motion does not exceed the absolute threshold value. *Benac et al.* [2004] described submerged notches in the northern Adriatic. Their results show well expressed but asymmetric tidal notches always submerged by at least 0.2 m indented between 0.18 – 1.50 m. These values range in the same order as our modelled notch estimates.

### 6.3 The role of coseismic displacements

The modelled cliff sections show the significant impact of the sea-level curve shape on time and duration of notch formation in accordance to a given constant coastal uplift/subsidence. Dependent on the shape of the sea-level curve the cliff morphology results from grazing, incising, and overwriting only from gradual climatically driven sea-level changes. When introducing coseismic activity to the model even more dynamics are addressed in the system. The abrupt migration of the erosional base potentially yields to the

development of an entirely new notch generation. However, in combination with an arcuate shaped erosional base height curve (Fig. 6) the migration is not oriented purely in one direction. Furthermore, repeated coseismic activity results not necessarily of the same migration stepsize since rates of a mean relative sea-level change vary from ascending (~6 kyr BP) to flat (~4 kyr BP), and also descending (~2 kyr BP). As a result, lower sections of a modern cliff face potentially formed the strandline at least two times since 7 kyr BP (Figs. 6a, b, c, and 12a).

In particular, modelled results for the southern Italian coastline show how repeated erosion modifies the developing cliff face (Fig. 8). When introducing coseismic displacements to the model, modification is even more apparent. Both scenarios where coseismic uplift was included indicate that coseismic offset possibly results in one of two options: I) rapid displacement of the erosional zone causing the development of an entirely new notch generation, which likely overprints older features to a greater or lesser degree (Fig. 13a), or II) prolonging or re-entering the erosive phase at a certain level in periods of gradual sea-level change (Fig. 12a). Furthermore, the scenario modelled for Heraion illustrates that a notch sequence on a modern cliff from top descending to sea-level is not inevitably of decreasing age caused by coseismic uplift events in periods of slightly uplift outpacing sea-level rise. Moreover, when rapid coseismically induced displacement prolongs the erosive phase the modern expression cannot be used to infer information about the specific event since it only causes deepening of the pre-existing notch.

### 6.4 Model versus reality

The reliability of both scenarios modelled for the western and eastern part of the Gulf of Corinth should not be overvalued due to idealized assumptions and generalizations according the applied sea-level curve. The two different scenarios of seismological history are applied since they pose results from different views. The inputs for the Heraion model are inferred from a study that aimed to directly investigate episodic uplift deduced from Holocene shorelines [*Pirazzoli et al.*, 1994]. The differences between model and natural cliff are most likely the result of the inherent model assumptions, a sea-level curve not specifically estimated for that region, and onshore tectonic activities which are not considered in the model (Fig. 14b). However, modelled tidal notches and minor indentation can be correlated to actual observations. For instance, notches modelled to +1.4 m and +2.8 m might coincide with observed expressions at +1.7 m and +3.1 m. Even depth relations between modelled and natural notches resemble each other in appearance. On the natural cliff the notch at +2.6 m forms the deepest indentation of the natural sequence which matches with the notch modelled to +2.0 m. In fact, no significant indentation is modelled in between these notches giving evidence for cumulative offsetting contributed by both, coseismic uplift and gradual relative sea-level change. However, balancing smaller coseismic uplift values from off-shore origin and down-throwing contributions from active on-shore faults potentially result in more paleo-strandlines than observed so far [*Schneiderwind et al.*, 2017].

The Eliki Fault scenario is based on the assumption of a regular seismic cycle with multiple coseismic uplift events each of 0.2-0.3 m [*Stewart & Vita-Finzi*, 1996]. Uplift values of this range and recurrence interval (not exceeding 1,000 years) are plausible and consistent with paleoseimological principles in extensional tectonic settings [*Jackson et al.*, 1982; *Papanikolaou et al.*, 2010]. The results for this scenario are more consistent with reports of the natural cliff face. *Stewart & Vita-Finzi* [1996] described prominent notch levels at +1.8 m dating to 1680 ± 130 years BP, and at +3.7 m dating to 2290 ± 115 years BP and 2600 ± 265 years BP. Varying dating results for the upper notch might be the consequence of repeated erosive phases compressed along a thin section of the cliff. In the modelled cliff a tidal notch

develops at +1.8 m as a consequence of coastal displacement at 1680 yrs BP and hence misses natural conformity only at one earthquake recurrence interval. The absence of a distinct erosive evidence for an earthquake that happened 1861 AD might be the consequence of an increasing amount of downward carving due to fluctuating gradients (relative sea-level and coastal uplift).

Therefore, our model shows promise for the potential reconstruction of actual cliff faces but needs better and more accurate input values for relative sea-level change and seismic history. However, in accordance with the assumptions made the algorithm combines the results from multiple disciplines and produces cliff faces that can be compared to natural exposures to support interpretation strategies. If the sea-level rise is well constrained, far range deglaciational effects are validated, and information about paleotectonic activity is available, a separation of spatial and temporary segments might be possible. However, to produce more reliable results parameters such as maximum overburden, lithological discontinuities, exposure to wave action, and much more have to be considered [*Trenhaile*, 2014]. Furthermore, constraining the erosional base does not only include isostatic corrected sea-levels but also tectonic activities on and offshore. In extensional Graben systems such as the Gulf of Corinth several coast-down-throwing normal faults on land potentially influence the erosional level. This research has implications for assessing the overall and local seismic activity of a certain region. Based on reasonable assumptions reliable information on overall tectonic activity as a budget and balanced structure-linked values can be gathered. Due to its simplicity the novel algorithm is transparent and reproducible increasing the objectivity in assessing coast-affecting tectonic activity.

## 7 Conclusion

Depending on the region and associated local sea-level history, Holocene tidal notches can form from 6,000-7,000 years BP in the Mediterranean Basin [see also *Trenhaile*, 2016]. Thereby, the very early stages of counterbalanced eustatic and isostatic conditions might not result in the most elevated sea-level marker at the present-day. In detail, modern cliff morphology contains indentations, nips, and deepened sections that are not true notches. This geomorphology is a product of continuous notch formation, repeated overprinting, bedrock heterogeniety, storm surge elevations. Gradual sea-level change optionally accompanied by tectonic activity shifts the erosional base along the vertical axis (see also Fig. 3). As a consequence, a notch sequence from top descending to sea-level does not necessarily adhere rigidly to and old-to-young chronology. Stages of almost-stagnation between regional sea-level rise and coastal uplift tend to produce more space between individual notch generations. However, resulting notch shapes appear widened in comparison to successively older features.

The developed algorithm is not as close to reality as required for a retro-deformation due to significant generalizations and simplifications. However, the model presented is the first that incorporates actual and region-specific Holocene sea-level changes, erosion rates, and landmass movements (slow and rapid). It points out how variable tidal notch development and preservation occurs even in local scale. Paleoseismological studies should benefit from its application since it provides a method for the evaluation of field observations and interpreted meanings. Case studies considering both coastal coseismic footwall uplift from offshore normal faults and coast downthrowing onshore faults could profit by evaluating the balance of relative motions.

In conclusion:

1. The algorithm makes clear how slow and rapid processes interplay and bias each other (modification)
2. The visualization illustrates how slow and gradual sea-level changes can result in sequences that look similar to those generated with influence of seismic activity
3. A notch offset exceeding several decimeters in a present-day notch sequence is not a contrariety to typical coseismic coastal footwall uplifts since recurrent overprinting and minor sea-level variation can produce such offsets even without tectonic activity. Therefore, tidal notches may not be used as primary earthquake geological effects without considering detailed sea-level history
4. Submerged notches can occur on emerging coastlines
5. "relative stagnation" is not a condition with absence of relative motion but comprises a scope of minor motion (<0.5 mm/yr) in dependency of the actual penetration period and erosion rate

The model presented enables researchers to have an enhanced understanding of the evolution of tidal notch sequences and points out how important reliable data of sea-level rise and coastal uplift are to the correct interpretation of such sequences.

**Acknowledgments**

T.M. Fernández-Steeger (RWTH Aachen University) is acknowledged for financial support and fruitful discussions. We thank the Editor Dr. Giovanni Coco and the Associate Editor Dr. Curt Storlazzi as well as Dr. Alan S. Trenhaile and an anonymous reviewer for their comments and suggestions, which significantly improved our manuscript. The data used are listed in the references. Supporting data are included as 10 video files in an SI file; any additional data may be obtained from S. Schneiderwind (email: s.schneiderwind@nug.rwth-aachen.de). Tide gauge data for figure 4a has been provided by the Hellenic Navy Hydrographic Service (HNHS). We note that there are no data sharing issues since all of the numerical information is provided in the figures produced by solving the equations in the paper.

**References**

Antonioli, F.; Ferranti, L.; Lambeck, K.; Kershaw, S.; Verrubbi, V.; Dai Pra, G. (2006): Late Pleistocene to Holocene record of changing uplift rates in southern Calabria and northeastern Sicily (southern Italy, Central Mediterranean Sea). In Tectonophysics 422 (1-4), pp. 23–40. DOI: 10.1016/j.tecto.2006.05.003.

Antonioli, F.; Lo Presti, V.; Rovere, A.; Ferranti, L.; Anzidei, M.; Furlani, S.; Mastronuzzi, G.; Orru, P.E.; Scicchitano, G.; Sannino, S.; Spampinato, C.R.; Palgiarulo, R.; Deiana, G.; de Sabata, E.; Sansó, P.; Vacchi, M.; Vecchio, A. (2015): Tidal notches in Mediterranean Sea: a comprehensive analysis. In Quaternary Science Reviews 119, pp. 66–84. DOI: 10.1016/j.quascirev.2015.03.016.

Armijo, R.; Meyer, B.; King, G. C. P.; Rigo, A.; Papanastassiou, D. (1996): Quaternary evolution of the Corinth Rift and its implications for the Late Cenozoic evolution of the Aegean. In Geophysical Journal International 126 (1), pp. 11–53. DOI: 10.1111/j.1365-246X.1996.tb05264.x.

Ayat, Berna (2013): Wave power atlas of Eastern Mediterranean and Aegean Seas. In Energy 54, pp. 251–262. DOI: 10.1016/j.energy.2013.02.060.

Benac, Č.; Juračić, M.; Bakran-Petricioli, T. (2004): Submerged tidal notches in the Rijeka Bay NE Adriatic Sea: indicators of relative sea-level change and of recent tectonic movements. In Marine Geology 212 (1-4), pp. 21–33. DOI: 10.1016/j.margeo.2004.09.002.

Besio, G.; Mentaschi, L.; Mazzino, A. (2016): Wave energy resource assessment in the Mediterranean Sea on the basis of a 35-year hindcast. In Energy 94, pp. 50–63. DOI: 10.1016/j.energy.2015.10.044.

Boulton, S. J.; Stewart, I. S. (2015): Holocene coastal notches in the Mediterranean region: Indicators of palaeoseismic clustering? In Geomorphology 237, pp. 29–37. DOI: 10.1016/j.geomorph.2013.11.012.

Carcaillet, J.; Mugnier, J. L.; Koçi, R.; Jouanne, F. (2009): Uplift and active tectonics of southern Albania inferred from incision of alluvial terraces. In Quaternary Research 71 (3), pp. 465–476. DOI: 10.1016/j.yqres.2009.01.002.

Carminati, E.; Doglioni, C.; Scrocca, D. (2003): Apennines subduction-related subsidence of Venice (Italy). In Geophys. Res. Lett. 30 (13), pp. n/a. DOI: 10.1029/2003GL017001.

Collier, R. E. L.; Leeder, M. R.; Rowe, P. J.; Atkinson, T. C. (1992): Rates of tectonic uplift in the Corinth and Megara Basins, central Greece. In Tectonics 11 (6), pp. 1159–1167. DOI: 10.1029/92TC01565.

Cooper, F.J.; Roberts, G.P.; Underwood, C.J. (2007): A comparison of 10 3 –10 5 year uplift rates on the South Alkyonides Fault, central Greece: Holocene climate stability and the formation of coastal notches. In Geophys. Res. Lett. 34 (14). DOI: 10.1029/2007GL030673.

Cundy, A.B.; Gaki-Papanastassiou, K.; Papanastassiou, D.; Maroukian, H.; Frogley, M. R.; Cane, T. (2010): Geological and geomorphological evidence of recent coastal uplift along a major Hellenic normal fault system (the Kamena Vourla fault zone, NW Evoikos Gulf, Greece). In Marine Geology 271 (1-2), pp. 156–164. DOI: 10.1016/j.margeo.2010.02.009.

Evelpidou, N.; Pirazzoli, P. A.; Vassilopoulos, A.; Tomasin, A. (2011a): Holocene submerged shorelines on Theologos area (Greece). In Zeitschrift für Geomorphologie 55 (1), pp. 31–44. DOI: 10.1127/0372-8854/2011/0055-0032.

Evelpidou, N.; Pirazzoli, P. A.; Saliège, J.-F.; Vassilopoulos, A. (2011b): Submerged notches and doline sediments as evidence for Holocene subsidence. In Continental Shelf Research 31 (12), pp. 1273–1281. DOI: 10.1016/j.csr.2011.05.002.

Evelpidou, N.; Vassilopoulos, A.; Pirazzoli, P. A. (2012a): Submerged notches on the coast of Skyros Island (Greece) as evidence for Holocene subsidence. In Geomorphology 141-142, pp. 81–87. DOI: 10.1016/j.geomorph.2011.12.025.

Evelpidou, N.; Kampolis, I.; Pirazzoli, P. A.; Vassilopoulos, A. (2012b): Global sea-level rise and the disappearance of tidal notches. In Global and Planetary Change 92-93, pp. 248–256. DOI: 10.1016/j.gloplacha.2012.05.013.

Evelpidou, Niki; Pirazzoli, Paolo Antonio; Spada, Giorgio (2015): Origin and Holocene Evolution of a Slightly Submerged Tidal Notch in the NE Adriatic. In Journal of Coastal Research 300, pp. 255–264. DOI: 10.2112/JCOASTRES-D-14-00016.1.

Evelpidou, N.; Pirazzoli, P. A. (2016): Estimation of the intertidal bioerosion rate from a well-dated fossil tidal notch in Greece. In Marine Geology. DOI: 10.1016/j.margeo.2016.04.017.

Faccenna, C.; Becker, T.W.; Auer, L.; Billi, A.; Boschi, L.; Brun, J.P.; Capitanio, F.A.; Funiciello, F.; Horvàth, F.; Jolivet, L.; Piromallo, C.; Royden, L.; Rossetti, F.; Serpelloni, E. (2014): Mantle dynamics in the Mediterranean. In Rev. Geophys. 52 (3), pp. 283–332. DOI: 10.1002/2013RG000444.

Ferranti, L.; Monaco, C.; Antonioli, F.; Maschio, L.; Kershaw, S.; Verrubbi, V. (2007): The contribution of regional uplift and coseismic slip to the vertical crustal motion in the Messina Straits, southern Italy: Evidence from raised Late Holocene shorelines. In J. Geophys. Res. 112 (B6). DOI: 10.1029/2006JB004473.

Furlani, S.; Cucchi, F. (2013): Downwearing rates of vertical limestone surfaces in the intertidal zone (Gulf of Trieste, Italy). In Marine Geology 343, pp. 92–98. DOI: 10.1016/j.margeo.2013.06.005.

Furlani, Stefano; Cucchi, Franco; Biolchi, Sara; Odorico, Roberto (2011): Notches in the Northern Adriatic Sea. Genesis and development. In Quaternary International 232 (1-2), pp. 158–168. DOI: 10.1016/j.quaint.2010.06.010.

Goodman-Tchernov, B.; Katz, O. (2015): Holocene-era submerged notches along the southern Levantine coastline: Punctuated sea level rise? In Quaternary International. DOI: 10.1016/j.quaint.2015.10.107.

Grützner, C.; Schneiderwind, S.; Papanikolaou, I.; Deligiannakis, G.; Pallikarakis, A.; Reicherter, K. (2016): New constraints on extensional tectonics and seismic hazard in northern Attica, Greece. The case of the Milesi Fault. In Geophysical Journal International 204 (1), pp. 180–199. DOI: 10.1093/gji/ggv443.

Harrison, R. W.; Tsiolakis, E.; Stone, B. D.; Lord, A.; McGeehin, J. P.; Mahan, S. A.; Chirico, P. (2013): Late Pleistocene and Holocene uplift history of Cyprus: implications for active tectonics along the southern margin of the Anatolian microplate. In Geological Society, London, Special Publications 372 (1), pp. 561–584. DOI: 10.1144/SP372.3.

Jackson, J. A.; Gagnepain, J.; Houseman, G.; King, G.C.P.; Papadimitriou, P.; Soufleris, C.; Virieux, J. (1982): Seismicity, normal faulting, and the geomorphological development of the Gulf of Corinth (Greece): the Corinth earthquakes of February and March 1981. In Earth and Planetary Science Letters 57 (2), pp. 377–397. DOI: 10.1016/0012-821X(82)90158-3.

Kelletat, D. H. (2005a): A Holocene Sea Level Curve for the Eastern Mediterranean from Multiple Indicators. In Z. Geomorph. N.F. 137, pp. 1–9.

Kelletat, D. H. (2005b): Notches. Encyclopedia of Coastal Science. Edited by M. L. Schwartz. Springer, Dordrecht.

Kershaw, S.; Guo, L. (2001): Marine notches in coastal cliffs: indicators of relative sea-level change, Perachora Peninsula, central Greece. In Marine Geology 179 (3-4), pp. 213–228. DOI: 10.1016/S0025-3227(01)00218-3.

Koukouvelas, I.; Mpresiakas, A.; Sokos, E.; Doutsos, T. (1996): The tectonic setting and earthquake ground hazards of the 1993 Pyrgos earthquake, Peloponnese, Greece. In Journal of the Geological Society 153 (1), pp. 39–49. DOI: 10.1144/gsjgs.153.1.0039.

Laborel, J.; Morhange, C.; Collina-Girard, J.; Laborel-Deguen, F. (1999): Littoral bioerosion, a tool for the study of sea level variations during the Holocene. In Bulletin of the Geological Society of Denmark 45, pp. 164–168.

Lambeck, K.; Antonioli, F.; Purcell, A.; Silenzi, S. (2004): Sea-level change along the Italian coast for the past 10,000yr. In Quaternary Science Reviews 23 (14-15), pp. 1567–1598. DOI: 10.1016/j.quascirev.2004.02.009.

Lambeck, K.; Purcell, A. (2005): Sea-level change in the Mediterranean Sea since the LGM: model predictions for tectonically stable areas. In Quaternary Science Reviews 24 (18-19), pp. 1969–1988. DOI: 10.1016/j.quascirev.2004.06.025.

Lambeck, K.; Rouby, H.; Purcell, A.; Sun, Y.; Sambridge, M. (2014): Sea level and global ice volumes from the Last Glacial Maximum to the Holocene. In Proceedings of the National Academy of Sciences of the United States of America 111 (43), pp. 15296–15303. DOI: 10.1073/pnas.1411762111.

Larson, M.P.; Sunamura, T.; Erikson, L.; Bayram, A.; Hanson, H. (2011): AN ANALYTICAL MODEL TO PREDICT DUNE AND CLIFF NOTCHING DUE TO WAVE IMPACT. In Int. Conf. Coastal. Eng. 1 (32). DOI: 10.9753/icce.v32.sediment.35.

Leeder, M. R.; McNeill, L. C.; Ll Collier, R. E.; Portman, C.; Rowe, P. J.; Andrews, J. E.; Gawthorpe, R. L. (2003): Corinth rift margin uplift: New evidence from Late Quaternary marine shorelines. In Geophys. Res. Lett. 30 (12), pp. n/a. DOI: 10.1029/2003GL017382.

Liberti, Luca; Carillo, Adriana; Sannino, Gianmaria (2013): Wave energy resource assessment in the Mediterranean, the Italian perspective. In Renewable Energy 50, pp. 938–949. DOI: 10.1016/j.renene.2012.08.023.

Martini, Paolo Marco de; Pantosti, Daniela; Palyvos, Nikolaos; Lemeille, Francis; McNeill, Lisa; Collier, Richard (2004): Slip rates of the Aigion and Eliki Faults from uplifted marine terraces, Corinth Gulf, Greece. In Comptes Rendus Geoscience 336 (4-5), pp. 325–334. DOI: 10.1016/j.crte.2003.12.006.

McNeill, L. C.; Collier, R.E.Ll. (2004): Uplift and slip rates of the eastern Eliki fault segment, Gulf of Corinth, Greece, inferred from Holocene and Pleistocene terraces. In Journal of the Geological Society 161 (1), pp. 81–92. DOI: 10.1144/0016-764903-029.

McNeill, L. C.; Cotterill, C. J.; Henstock, T. J.; Bull, J. M.; Stefatos, A.; Collier, R.E.Ll. et al. (2005): Active faulting within the offshore western Gulf of Corinth, Greece: Implications for models of continental rift deformation. In Geol 33 (4), p. 241. DOI: 10.1130/G21127.1.

Papanikolaou, D.; Papanikolaou, I. (2007): Geological, geomorphological and tectonic structure of NE Attica and seismic hazard implications for the northern edge of the Athens plain. In Bulletin of the Geological Society of Greece 40, pp. 425–438.

Papanikolaou, D.; Royden, L. H. (2007): Disruption of the Hellenic arc: Late Miocene extensional detachment faults and steep Pliocene-Quaternary normal faults-Or what happened at Corinth? In Tectonics 26 (5), TC5003. DOI: 10.1029/2006TC002007.

Papanikolaou, D. J. (1984): The three metamorphic belts of the Hellenides. A review and a kinematic interpretation. In Geological Society, London, Special Publications 17 (1), pp. 551–561. DOI: 10.1144/GSL.SP.1984.017.01.42.

Papanikolaou, I. D.; Foumelis, M.; Parcharidis, I.; Lekkas, E. L.; Fountoulis, I. G. (2010): Deformation pattern of the 6 and 7 April 2009, MW=6.3 and MW=5.6 earthquakes in L'Aquila (Central Italy) revealed by ground and space based observations. In Nat. Hazards Earth Syst. Sci. 10 (1), pp. 73–87. DOI: 10.5194/nhess-10-73-2010.

Papanikolaou, I. D.; Roberts, G. P.; Michetti, A. M. (2005): Fault scarps and deformation rates in Lazio–Abruzzo, Central Italy: Comparison between geological fault slip-rate and GPS data. In Tectonophysics 408 (1-4), pp. 147–176. DOI: 10.1016/j.tecto.2005.05.043.

Pirazzoli, P. A. (1986): Marine notches. In Orson van de Plassche (Ed.): Sea-Level Research. Dordrecht: Springer Netherlands, pp. 361–400.

Pirazzoli, P. A. (1991): World atlas of Holocene sea-level changes. Amsterdam, New York: Elsevier (Elsevier oceanography series, 58).

Pirazzoli, P. A.; Laborel, J.; Saliège, J. F.; Erol, O.; Kayan, İ.; Person, A. (1991): Holocene raised shorelines on the Hatay coasts (Turkey): Palaeoecological and tectonic implications. In Marine Geology 96 (3-4), pp. 295–311. DOI: 10.1016/0025-3227(91)90153-U.

Pirazzoli, P. A.; Montaggioni, L. F.; Saliège, J. F.; Segonzac, G.; Thommeret, Y.; Vergnaud-Grazzini, C. (1989): Crustal block movements from Holocene shorelines: Rhodes Island (Greece). In Tectonophysics 170 (1-2), pp. 89–114. DOI: 10.1016/0040-1951(89)90105-4.

Pirazzoli, P. A.; Stiros, S. C.; Arnold, M.; Laborel, J.; Laborel-Deguen, F.; Papageorgiou, S. (1994): Episodic uplift deduced from Holocene shorelines in the Perachora Peninsula, Corinth area, Greece. In Tectonophysics 229 (3-4), pp. 201–209. DOI: 10.1016/0040-1951(94)90029-9.

Pirazzoli, P. A.; Thommeret, J.; Thommeret, Y.; Laborel, J.; Montag-Gioni, L. F. (1982): Crustal block movements from holocene shorelines: Crete and Antikythira (Greece). In Tectonophysics 86 (1-3), pp. 27–43. DOI: 10.1016/0040-1951(82)90060-9.

Pirazzoli, Paolo A.; Evelpidou, Niki (2013): Tidal notches: A sea-level indicator of uncertain archival trustworthiness. In Palaeogeography, Palaeoclimatology, Palaeoecology 369, pp. 377–384. DOI: 10.1016/j.palaeo.2012.11.004.

Porter, Neil J.; Trenhaile, Alan S.; Prestanski, Kyle; Kanyaya, Jacob I. (2010): Patterns of surface downwearing on shore platforms in eastern Canada. In Earth Surf. Process. Landforms 35 (15), pp. 1793–1810. DOI: 10.1002/esp.2018.

Queffeulou, Pierre; Bentamy, Abderrahim (2007): Analysis of Wave Height Variability Using Altimeter Measurements. Application to the Mediterranean Sea. In J. Atmos. Oceanic Technol. 24 (12), pp. 2078–2092. DOI: 10.1175/2007JTECH0507.1.

Roberts, G. G.; White, N. J.; Shaw, B. (2013): An uplift history of Crete, Greece, from inverse modeling of longitudinal river profiles. In Geomorphology 198, pp. 177–188. DOI: 10.1016/j.geomorph.2013.05.026.

Roberts, G. P.; Houghton, S. L.; Underwood, C.; Papanikolaou, I.; Cowie, P. A.; van Calsteren, P.; Wigley, T.; Cooper, F.J.; McArthur, J.M. (2009): Localization of Quaternary slip rates in an active rift in 10 5 years: An example from central Greece constrained by 234 U- 230 Th coral dates from uplifted paleoshorelines. In J. Geophys. Res. 114 (B10). DOI: 10.1029/2008JB005818.

Rust, D.; Kershaw, S. (2000): Holocene tectonic uplift patterns in northeastern Sicily: evidence from marine notches in coastal outcrops. In Marine Geology 167 (1-2), pp. 105–126. DOI: 10.1016/S0025-3227(00)00019-0.

Sakellariou, D.; Lykousis, V.; Alexandri, S.; Kaberi, H.; Rousakis, G.; Nomikou, P. et al. (2007): Faulting, seismic-stratigraphic architecture and Late Quaternary evolution of the Gulf of Alkyonides Basin? East Gulf of Corinth, Central Greece. In Basin Research 19 (2), pp. 273–295. DOI: 10.1111/j.1365-2117.2007.00322.x.

Schildgen, T. F.; Cosentino, D.; Bookhagen, B.; Niedermann, S.; Yıldırım, C.; Echtler, H.; Wittmann, H.; Strecker, M.R. (2012): Multi-phased uplift of the southern margin of the Central Anatolian plateau, Turkey: A record of tectonic and upper mantle processes. In Earth and Planetary Science Letters 317-318, pp. 85–95. DOI: 10.1016/j.epsl.2011.12.003.

Schneiderwind, S.; Boulton, S. J.; Papanikolaou, I.; Reicherter, K. (2017): Innovative tidal notch detection using TLS and fuzzy logic. Implications for palaeo-shorelines from compressional (Crete) and extensional (Gulf of Corinth) tectonic settings. In Geomorphology 283, pp. 189–200. DOI: 10.1016/j.geomorph.2017.01.028.

Serpelloni, E.; Faccenna, C.; Spada, G.; Dong, D.; Williams, S.D.P. (2013): Vertical GPS ground motion rates in the Euro-Mediterranean region: New evidence of velocity gradients at different spatial scales along the Nubia-Eurasia plate boundary. In J. Geophys. Res. Solid Earth 118 (11), pp. 6003–6024. DOI: 10.1002/2013JB010102.

Sivan, D.; Lambeck, K.; Toueg, R.; Raban, A.; Porath, Y.; Shirman, B. (2004): Ancient coastal wells of Caesarea Maritima, Israel, an indicator for relative sea level changes during the last 2000 years. In Earth and Planetary Science Letters 222 (1), pp. 315–330. DOI: 10.1016/j.epsl.2004.02.007.

Sivan, D.; Wdowinski, S.; Lambeck, K.; Galili, E.; Raban, A. (2001): Holocene sea-level changes along the Mediterranean coast of Israel, based on archaeological observations and numerical model. In Palaeogeography, Palaeoclimatology, Palaeoecology 167 (1-2), pp. 101–117. DOI: 10.1016/S0031-0182(00)00234-0.

Stewart, I. S.; Cundy, A.; Kershaw, S.; Firth, C. (1997): Holocene coastal uplift in the taormina area, northeastern sicily: Implications for the southern prolongation of the calabrian seismogenic belt. In Journal of Geodynamics 24 (1-4), pp. 37–50. DOI: 10.1016/S0264-3707(97)00012-4.

Stewart, I.; Vita-Finzi, C. (1996): Coastal uplift on active normal faults: The Eliki Fault, Greece. In Geophys. Res. Lett. 23 (14), pp. 1853–1856. DOI: 10.1029/96GL01595.

Stiros, S. C.; Laborel, J.; Laborel-Deguen, F.; Papageorgiou, S.; Evin, J.; Pirazzoli, P. A. (2000): Seismic coastal uplift in a region of subsidence: Holocene raised shorelines of Samos Island, Aegean Sea, Greece. In Marine Geology 170 (1-2), pp. 41–58. DOI: 10.1016/S0025-3227(00)00064-5.

Stocchi, P.; Spada, G.; Cianetti, S. (2005): Isostatic rebound following the Alpine deglaciation: impact on the sea level variations and vertical movements in the Mediterranean region. In Geophysical Journal International 162 (1), pp. 137–147. DOI: 10.1111/j.1365-246X.2005.02653.x.

Tortorici, L.; Monaco, C.; Tansi, C.; Cocina, O. (1995): Recent and active tectonics in the Calabrian arc (Southern Italy). In Tectonophysics 243 (1-2), pp. 37–55. DOI: 10.1016/0040-1951(94)00190-K.

Torunski, H. (1979): Biological erosion and its significance for the morphogenesis of limestone coasts and for nearshore sedimentation (Northern Ardriatic). In Senckenberg. Marit. 11, pp. 193–265.

Trenhaile, A. S.; Mercan, D. W. (1984): Frost weathering and the saturation of coastal rocks. In Earth Surf. Process. Landforms 9 (4), pp. 321–331. DOI: 10.1002/esp.3290090405.

Trenhaile, A. S. (2014): Modelling tidal notch formation by wetting and drying and salt weathering. In Geomorphology 224, pp. 139–151. DOI: 10.1016/j.geomorph.2014.07.014.

Trenhaile, A. S. (2015): Coastal notches. Their morphology, formation, and function. In Earth-Science Reviews 150, pp. 285–304. DOI: 10.1016/j.earscirev.2015.08.003.

Trenhaile, A. S. (2016): Modelling coastal notch morphology and developmental history in the Mediterranean. In GeoResJ 9-12, pp. 77–90. DOI: 10.1016/j.grj.2016.09.003.

Westaway, R. (1993): Quaternary uplift of southern Italy. In J. Geophys. Res. 98 (B12), p. 21741. DOI: 10.1029/93JB01566.

Westaway, R.; Pringle, M.; Yurtmen, S.; Demir, T.; Bridgland, D.; Rowbotham, G.; Maddy, D. (2004): Pliocene and Quaternary regional uplift in western Turkey: the Gediz River terrace staircase and the volcanism at Kula. In Tectonophysics 391 (1-4), pp. 121–169. DOI: 10.1016/j.tecto.2004.07.013.

Wöppelmann, G.; Marcos, M. (2012): Coastal sea level rise in southern Europe and the nonclimate contribution of vertical land motion. In J. Geophys. Res. 117 (C1), pp. n/a. DOI: 10.1029/2011JC007469.

Zazo, C.; Silva, P.G; Goy, J.L; Hillaire-Marcel, C.; Ghaleb, B.; Lario, J.; Bardají, T.; González, A. (1999): Coastal uplift in continental collision plate boundaries: data from the Last Interglacial marine terraces of the Gibraltar Strait area (south Spain). In Tectonophysics 301 (1-2), pp. 95–109. DOI: 10.1016/S0040-1951(98)00217-0.

Zazo, C.; Goy, J.L.; Dabrio, C.J.; Bardají, T.; Hillaire-Marcel, C.; Ghaleb, B.; González-Delgado, J.-Á.; Soler, V. (2003): Pleistocene raised marine terraces of the Spanish Mediterranean and Atlantic coasts: records of coastal uplift, sea-level highstands and climate changes. In Marine Geology 194 (1-2), pp. 103–133. DOI: 10.1016/S0025-3227(02)00701-6.

Table 1. Applied input parameters for different regions. SLC = source of the sea-level curve. CAP = central Anatolian Plateau.

| | SLC | Tidal range | Vertical motion | EQ? | Erosion rate | Cliff |
|---|---|---|---|---|---|---|
| W. Gulf of Corinth, Greece | *Lambeck & Purcell*, 2005 | 0.3 m | (+) 1.2 mm/yr | no | 0.5 mm/yr | 90° |
| E. Gulf of Corinth, Greece | *Lambeck & Purcell*, 2005 | 0.3 m | (+) 0.6 mm/yr | no | 0.5 mm/yr | 90° |
| E. Sicily and Calabria, Italy | *Lambeck et al.*, 2004 | 0.3 m | (+) 1.0 mm/yr | no | 0.5 mm/yr | 90° |
| Tuscan Coast, Italy | *Lambeck & Purcell*, 2005 | 0.3 m | (+) 0.2 mm/yr | no | 0.5 mm/yr | 90° |
| S. margin of the CAP, Turkey | *Lambeck*, 1995 | 0.3 m | (+) 0.7 mm/yr | no | 0.5 mm/yr | 90° |
| Carmel Coast, Israel | *Lambeck & Purcell*, 2005 | 0.3 m | (+) 0.1 mm/yr | no | 0.5 mm/yr | 90° |
| N. Adria, Italy | *Lambeck et al.*, 2004 | 0.3 m | (-) 0.35 mm/yr | no | 0.5 mm/yr | 90° |
| Samos Island, Greece | *Lambeck*, 1995 | 0.3 m | (+) 0.6 mm/yr | no | 0.5 mm/yr | 90° |

Table 2. Input of coseismic parameter (dates in bold numbers). *Pirazzoli et al.* [1994] dated three notches at Heraion and identified a fourth generation at 1.7 m (asl). *Stewart & Vita-Finzi* [1996] dated two shorelines at the Eliki fault in the western Gulf of Corinth and estimated 0.2-0.3 m coseismic uplift per event.

| | # | elevation [m] | dated to | coseismic uplift [m] |
|---|---|---|---|---|
| Heraion, Perachora Peninsula | 1 | 3.2 | **4380** ± 60 BP | 0.6 |
| | 2 | 2.6 | **2350** ± 90 BP | 0.9 |
| | 3 | 1.7 | ND (**1333 BP**) | 0.6 |
| | 4 | 1.1 | **315** ± 125 BP | 1.1 |
| | | | | |
| Eliki, w. Gulf of Corinth | 1 | - | ND (**7352 BP**) | 0.25 |
| | 2 | - | ND (**6643 BP**) | 0.2 |
| | 3 | - | ND (**5934 BP**) | 0.3 |
| | 4 | - | ND (**5225 BP**) | 0.28 |
| | 5 | - | ND (**4516 BP**) | 0.22 |
| | 6 | - | ND (**3807 BP**) | 0.25 |
| | 7 | - | ND (**3098 BP**) | 0.22 |
| | 8 | 3.7 | 2290 ± 115 BP<br>2600 ± 265 BP<br>**2389** BP | 0.23 |
| | 9 | 1.8 | **1680** ± 130 BP | 0.25 |
| | 10 | - | ND (**831 BP**) | 0.26 |
| | 11 | - | **89** BP | 0.26 |

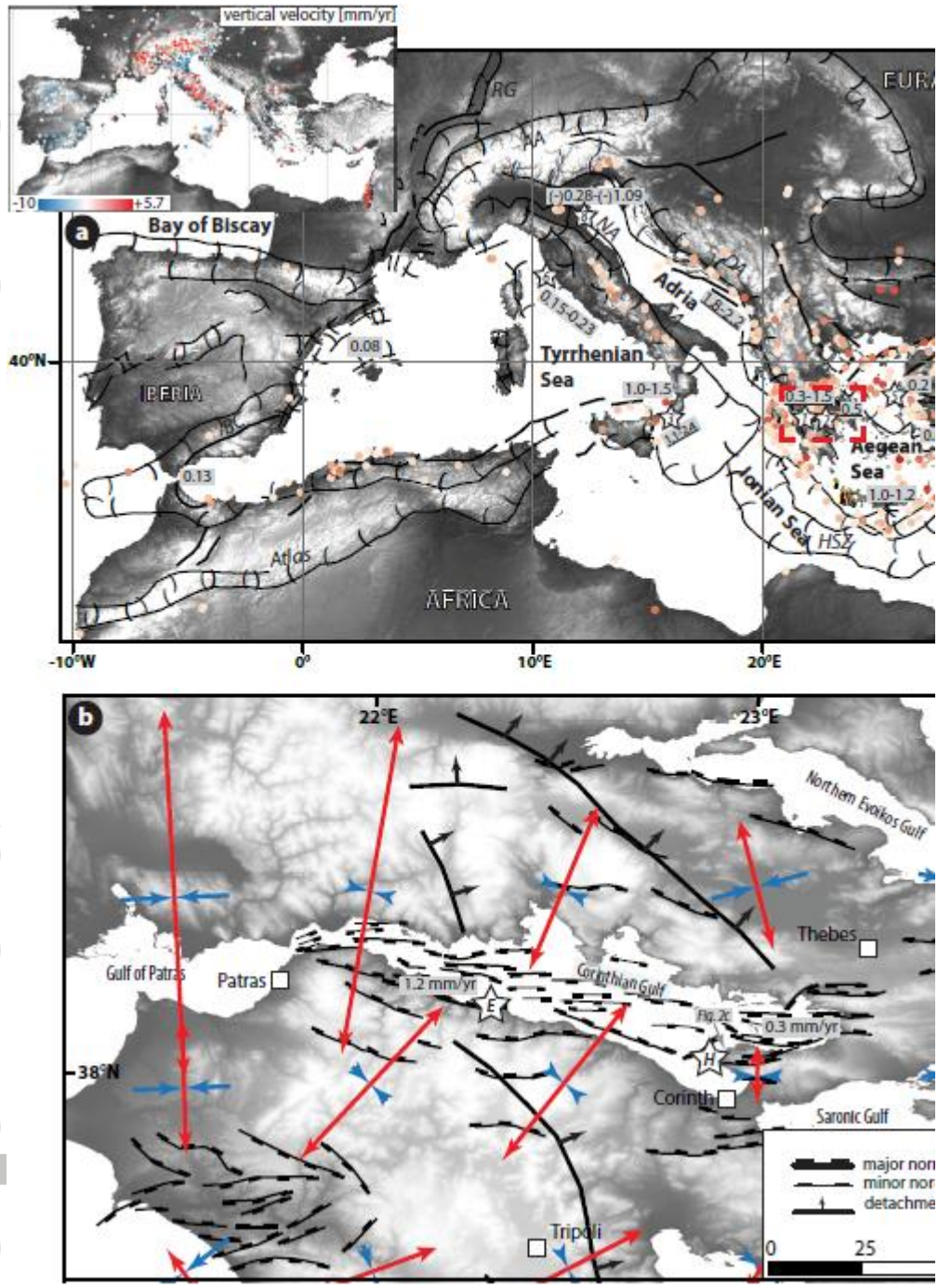


**Figure 1**. Study areas throughout the Mediterranean. a) Plate tectonic setting of the Mediterranean [modified after *Faccenna et al.*, 2014]. Inset shows vertical motion velocity derived from continuous GPS stations provided by *Serpelloni et al.* [2013]. Obvious coherent patterns of uplift (e.g. Alps) and subsidence (e.g. Spain) demonstrate the tremendous diversity of the Mediterranean geodetic field. *Boulton & Stewart* [2015] provided a database on tidal notches (rectangles) in the eastern Mediterranean basin. Estimates on regional and local uplift rates range across from -1.09 – 2.4 mm/yr [*Collier et al.*, 1992; *Westaway*, 1993; *Stewart & Vita-Finzi*, 1996; *Stewart et al.*, 1997; *Zazo et al.*, 1999; *Stiros et al.*, 2000; *Sivan et al.*, 2001; *Leeder et al.*, 2003; *Zazo et al.*, 2003; *Lambeck et al.*, 2004; *McNeill & Collier*, 2004; *Westaway et al.*, 2004; *Antonioli et al.*, 2006; *Cooper et al.*, 2007; *Ferranti et al.*, 2007; *Carcaillet et al.*, 2009; *Roberts et al.*, 2009; *Cundy et al.*, 2010; *Schildgen et al.*, 2012;

*Roberts & Shaw*, 2013; *Harrison et al.*, 2016]. Stars indicate test regions: (1) western Gulf of Corinth, (2) eastern Gulf of Corinth, (3) eastern Sicily and Calabria, (4) southern margin of the central Anatolian Plateau, (5) Samos Island, (6) Tuscan coast, (7) Carmel Coast, and (8) northern Adriatic. Earthquake (EQ) data covering < 500 events (1905-2015) with a maximum focal depth of 20 km is provided by the USGS. AA = Alpine Arc, DA = Dinaric Alps, CA = Carpathian Arc, BC = Betic Cordilleras, HSZ = Hellenic Subduction Zone, NA = Northern Adriatic, NAF = North Anatolian Fault, RG = Rhine Graben. Red box indicates extents of b. b) Geodynamics of central Greece. Faults were compiled from *Koukouvelas et al.* [1996], *Papanikolaou & Papanikolaou* [2007], *Papanikolaou & Royden* [2007], *Sakellariou et al.* [2007], *Roberts et al.* [2009], and *Grützner et al.* [2016]. Strain rates are from *Hollenstein et al.* [2008]. Stars indicate the location of the test sites for model comparison with actual cliff faces from the Eliki fault (E) and Cape Heraion (H).

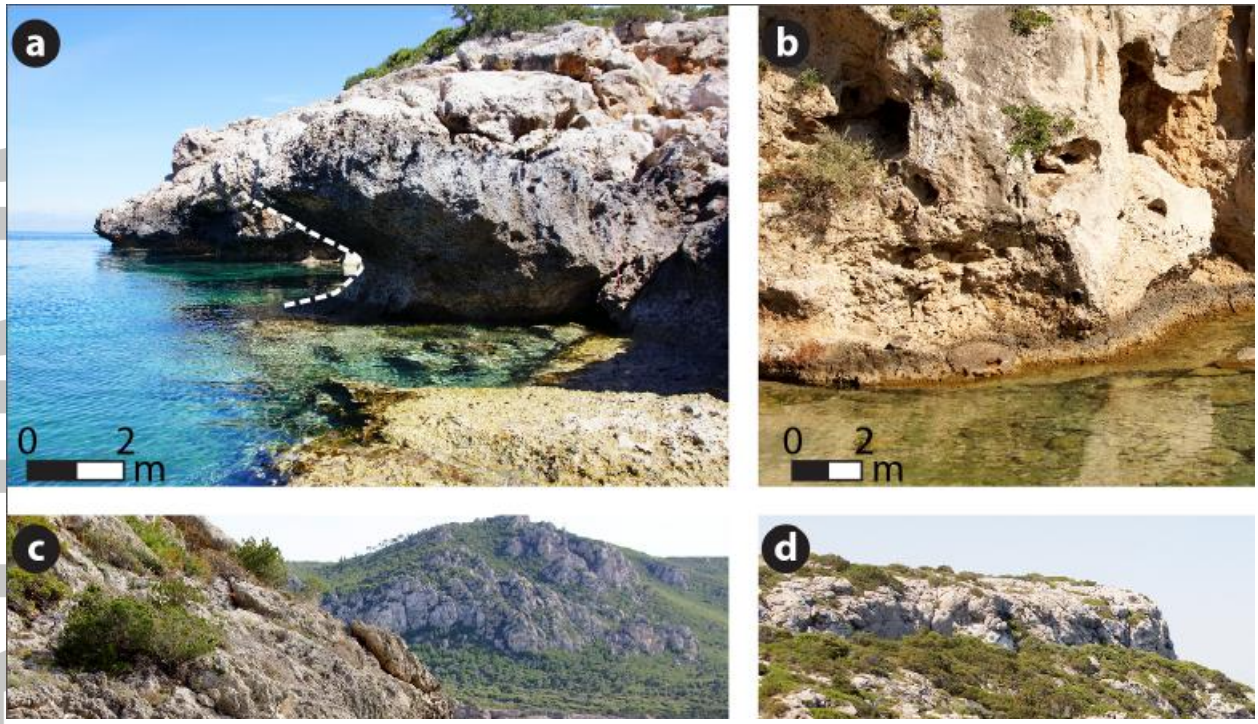


**Figure 2**. Examples for deeply incised notches withstanding cliff collapse in the Mediterranean. Thick-bedded Triassic – Lower Jurassic neritic limestones belonging to the Beotia Unit along the coast of the Perachora Peninsula (eastern Corinthian Gulf, Greece) can support the overburden even when incised up to ~2 m. Profiles are indicated by white dashed lines. a) and d) show raised shorelines closely located to Cape Heraion. b) A sequence of different raise shorelines also at Cape Heraion. c) Incised Cliff at Sterna (see Fig. 1b).

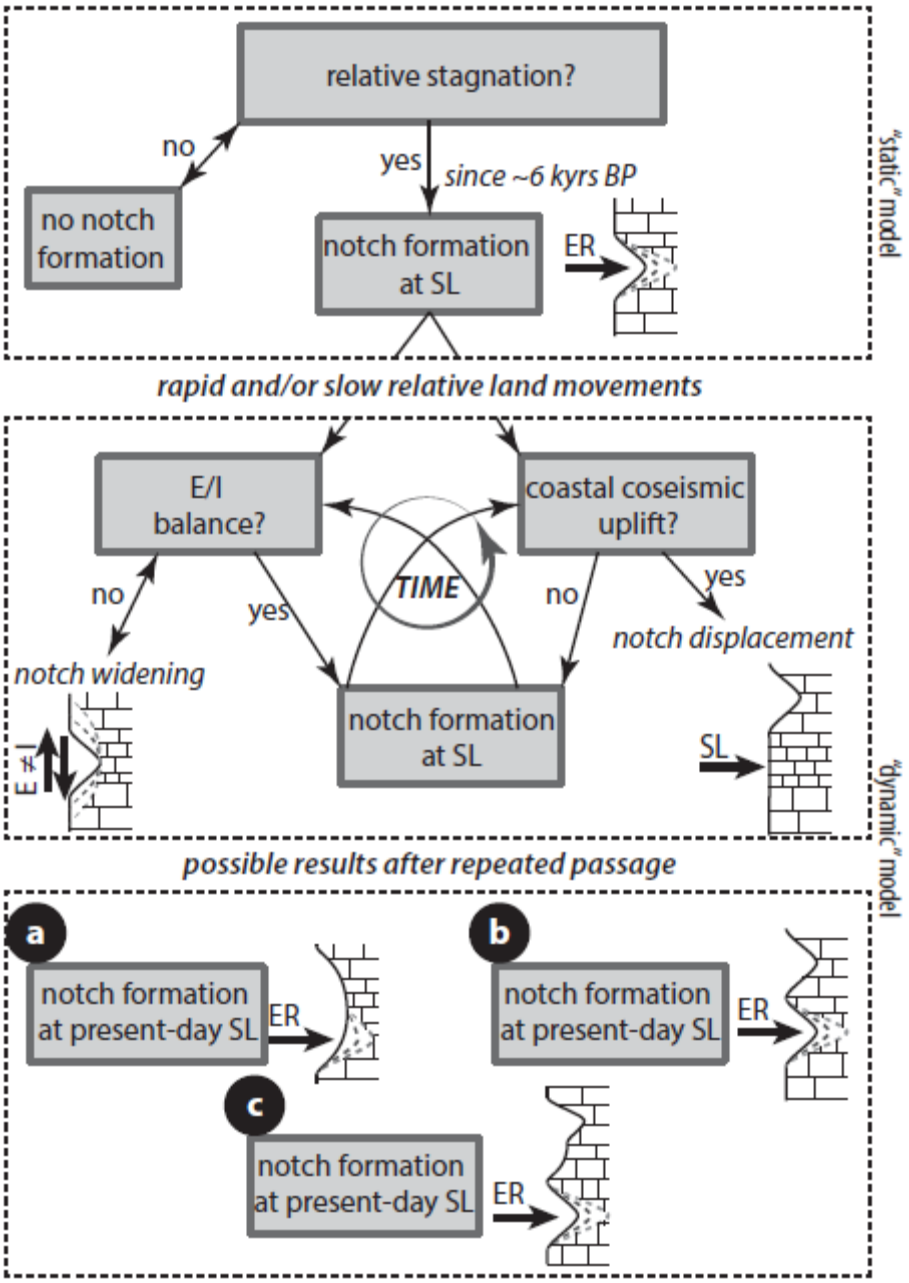


**Figure 3**. Logic tree for tidal notch sequence evolution. The static notch formation model incorporates only the erosion rate (ER) to estimate the notch depth. The dynamic model considers gradual sea-level (SL) changes due to unbalanced eustasy (E) and isostasy (I), and coseismic land displacements. Resulting cliff shapes contain widened notches (a), emerged notches (b), or a combination of all that (c).

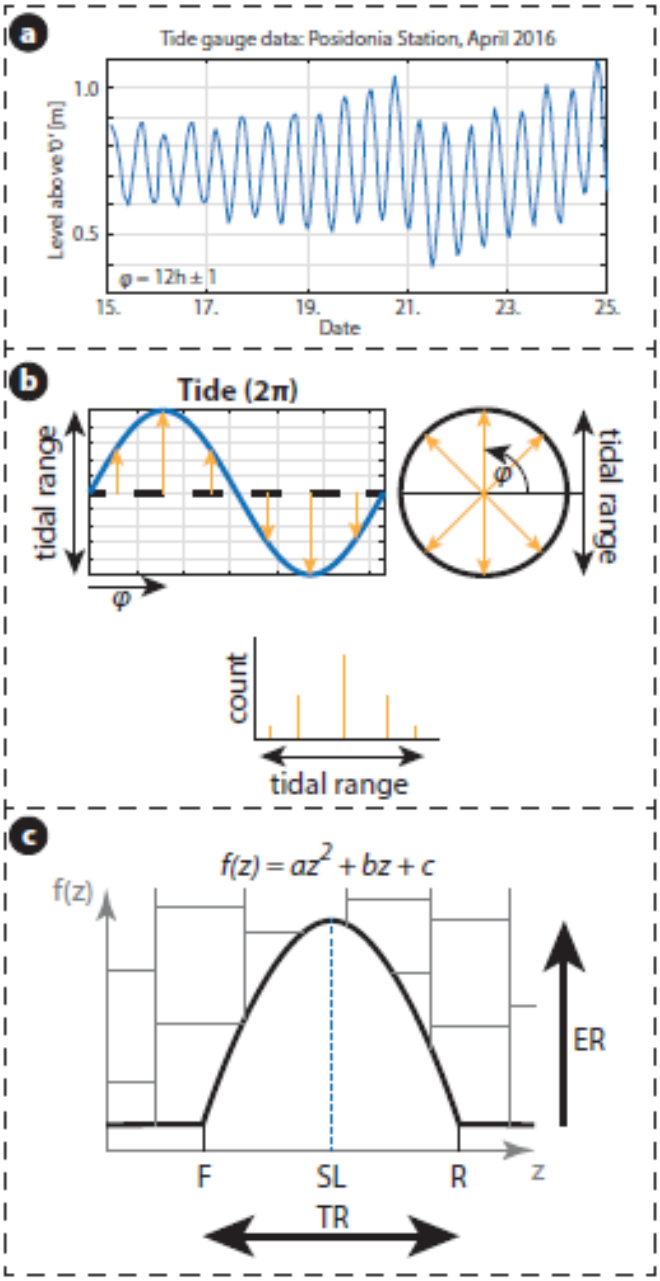


**Figure 4**. Assumptions leading to a quadric polynomial to cover requirements of tidal notch shape description: a) actual tide gauge data from April 2016 for the eastern Gulf of Corinth provided by the Hellenic Navy Hydrographic Service. φ is the tide period. b) the diurnal tide equals a sine function in a long-term average. Plotted into an unit cycle the moment φ depicts an angle pointing to an associated height within the tidal range. Each height depicts a bin in the histogram plot; c) a quadric polynomial describing the depth f(z) along a symmetrical notch profile. Floor (F) and roof (R) depict the roots separated by the tidal range (TR) along the x-axis. Note, the x-axis is labeled as 'z' for a better understanding since it represents the vertical orientation of the cliff face. The erosion rate (ER) corresponds to c and determines the depth of the notch after one year.

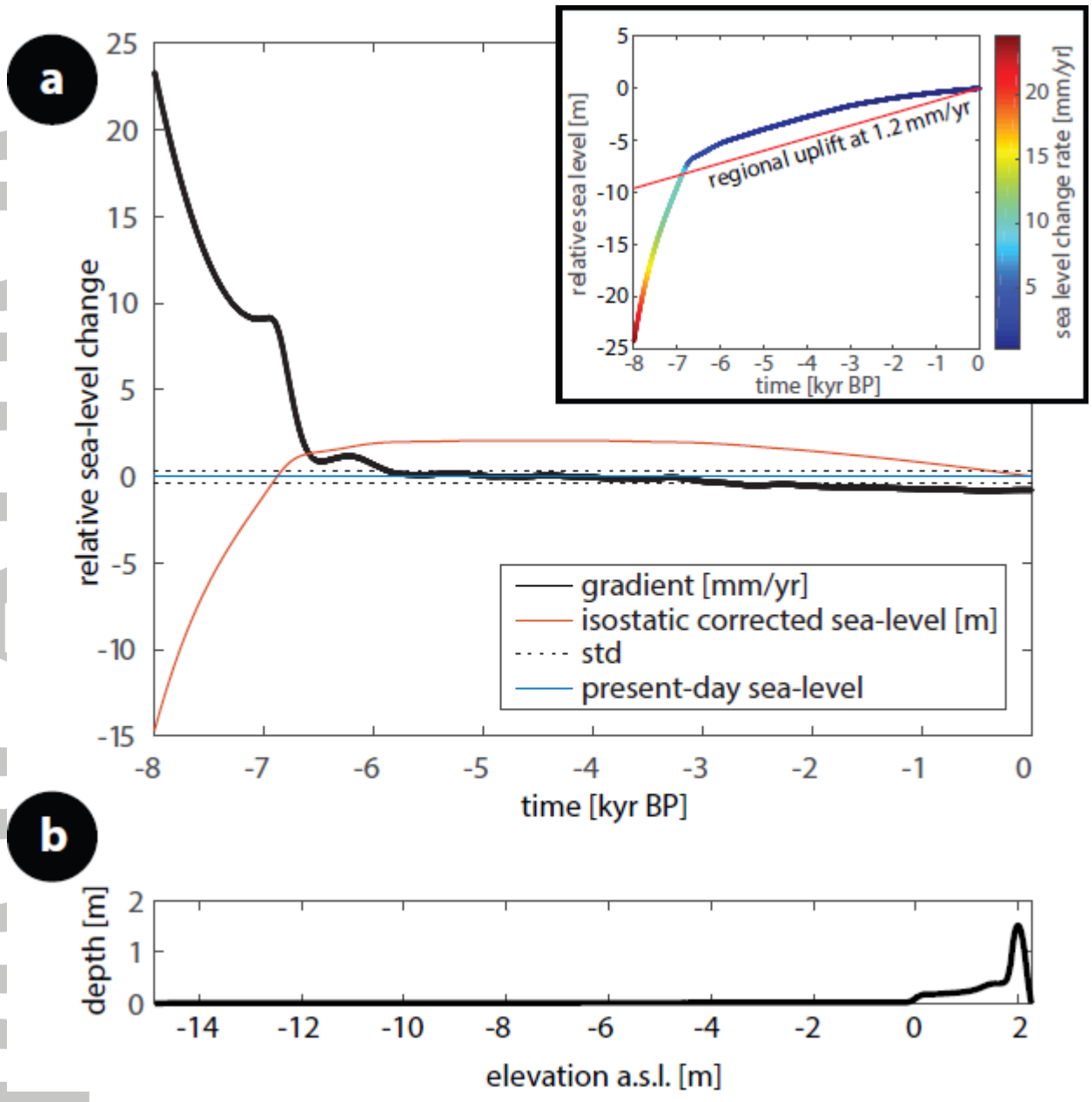


**Figure 5**. Applied sea-level curve and coastal uplift (inset graph) resulting in tidal notches: a) sea-level curve [e.g. *Lambeck & Purcell*, 2005] corrected for coastal uplift; b) resulting notch sequence.

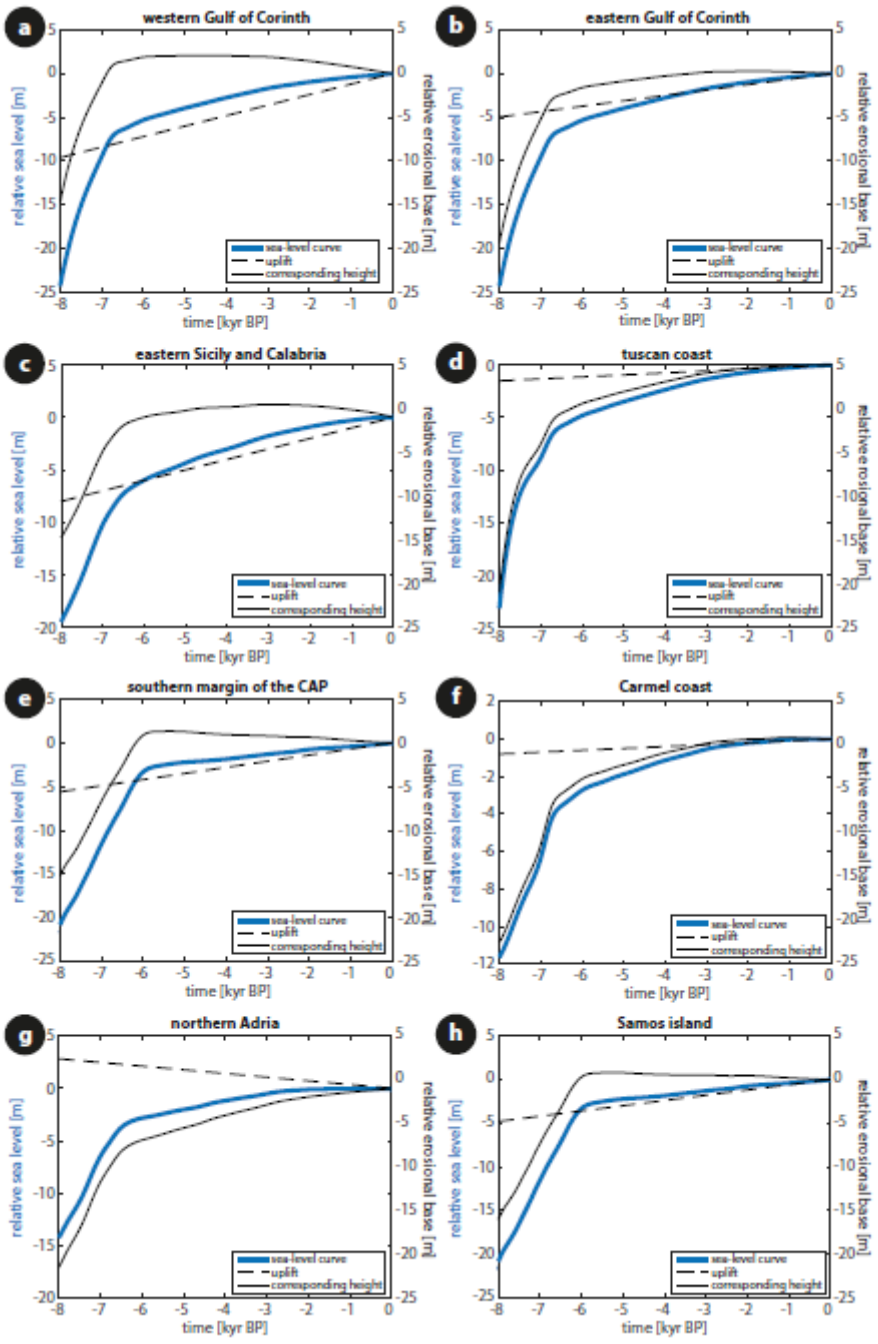


**Figure 6**. Sea-level curves and uplift trend corrected erosional bases corresponding to todays' sea-level datum. Regions in Greece and Italy experience > 1 mm/yr coastal uplift (a-c). (d-f and h) These regions represent areas of minor uplift. The northern Adriatic coast has continuously subsided since the last glacial maximum (g).

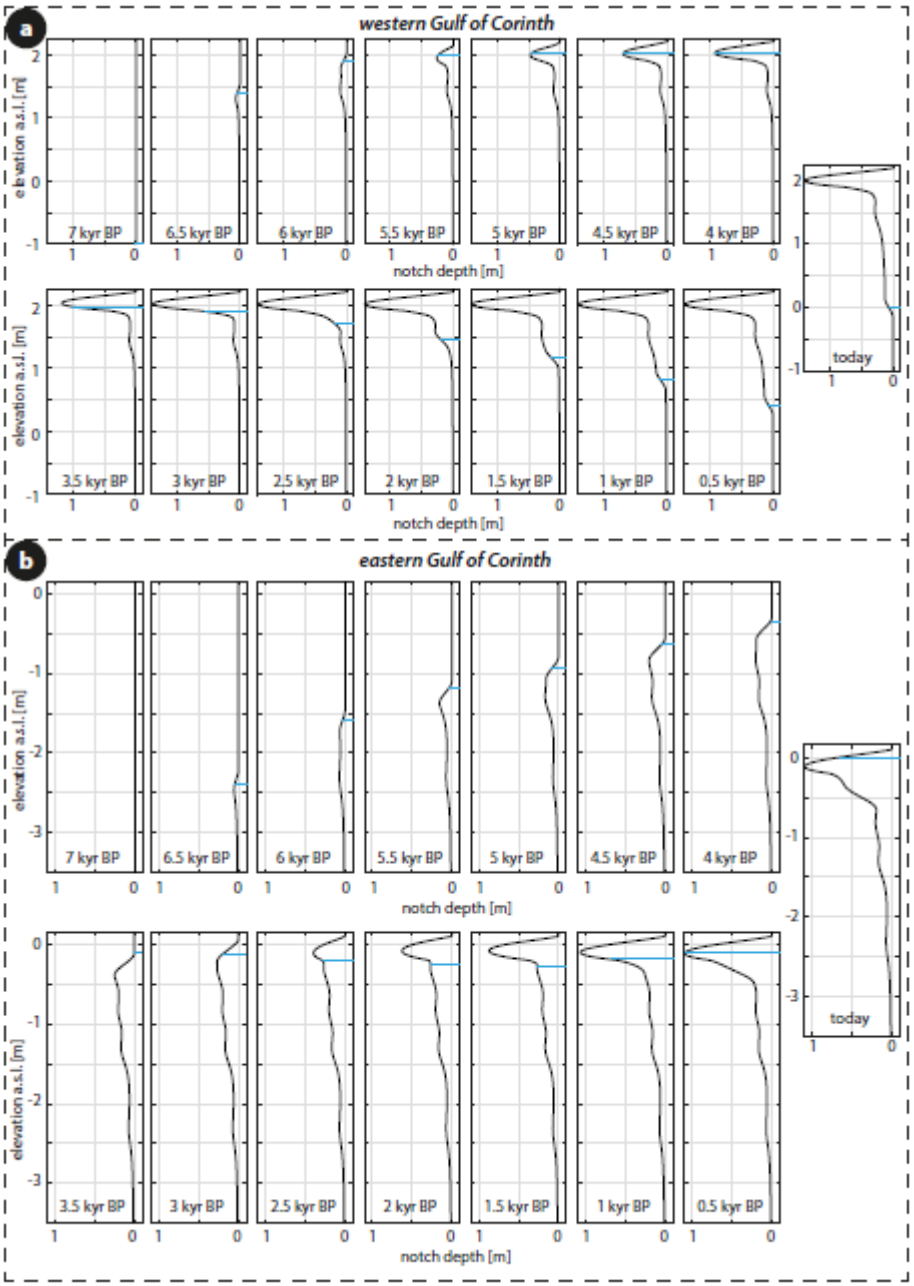


**Figure 7**. Time slices of tidal notch development on rapidly emerging coastlines such as the western Gulf of Corinth (a) and its eastern part accompanied by moderate emergence (b). Blue lines indicate sea-level at that time.

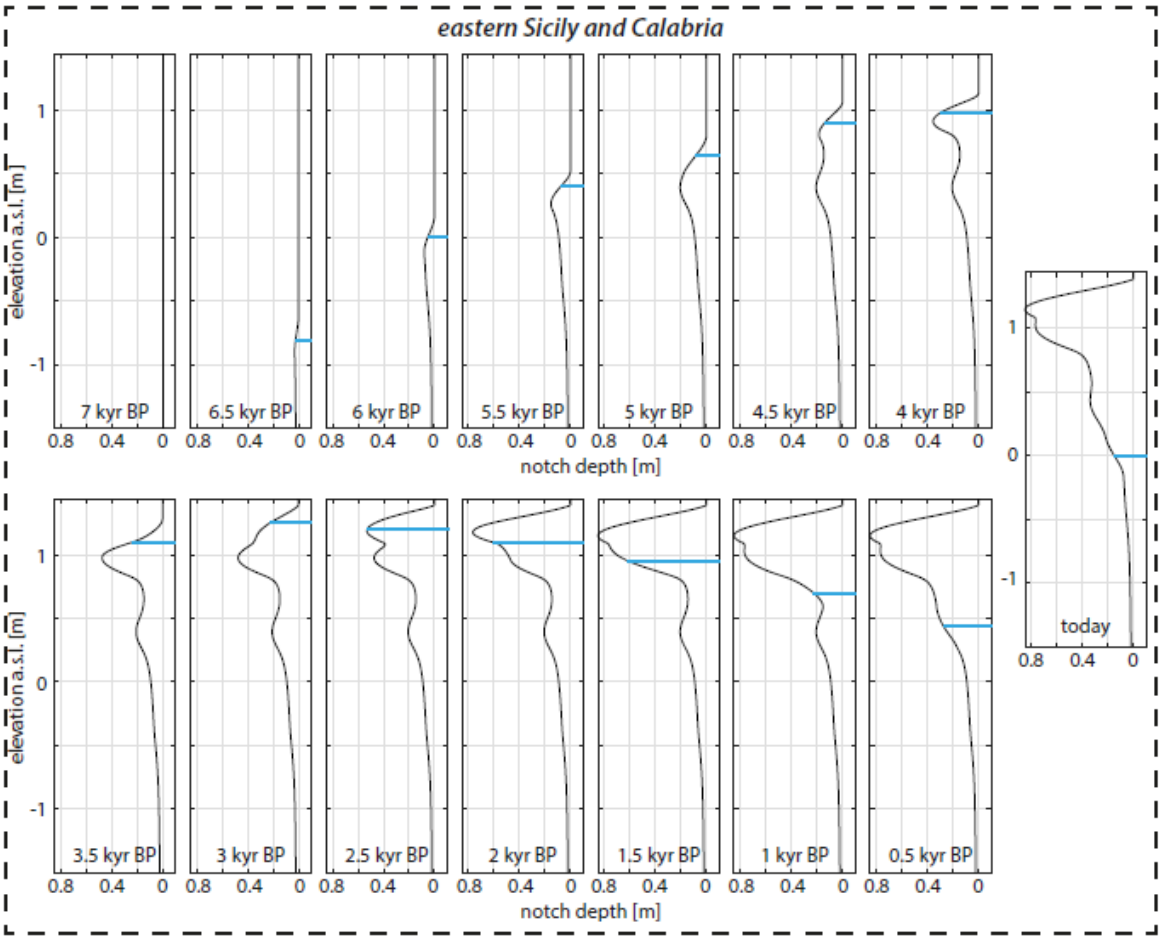


**Figure 8**. Simulated notch formation time slices for eastern Sicily and Calabria which pose examples for moderately emerging coasts. Blue lines indicate sea-level at that time.

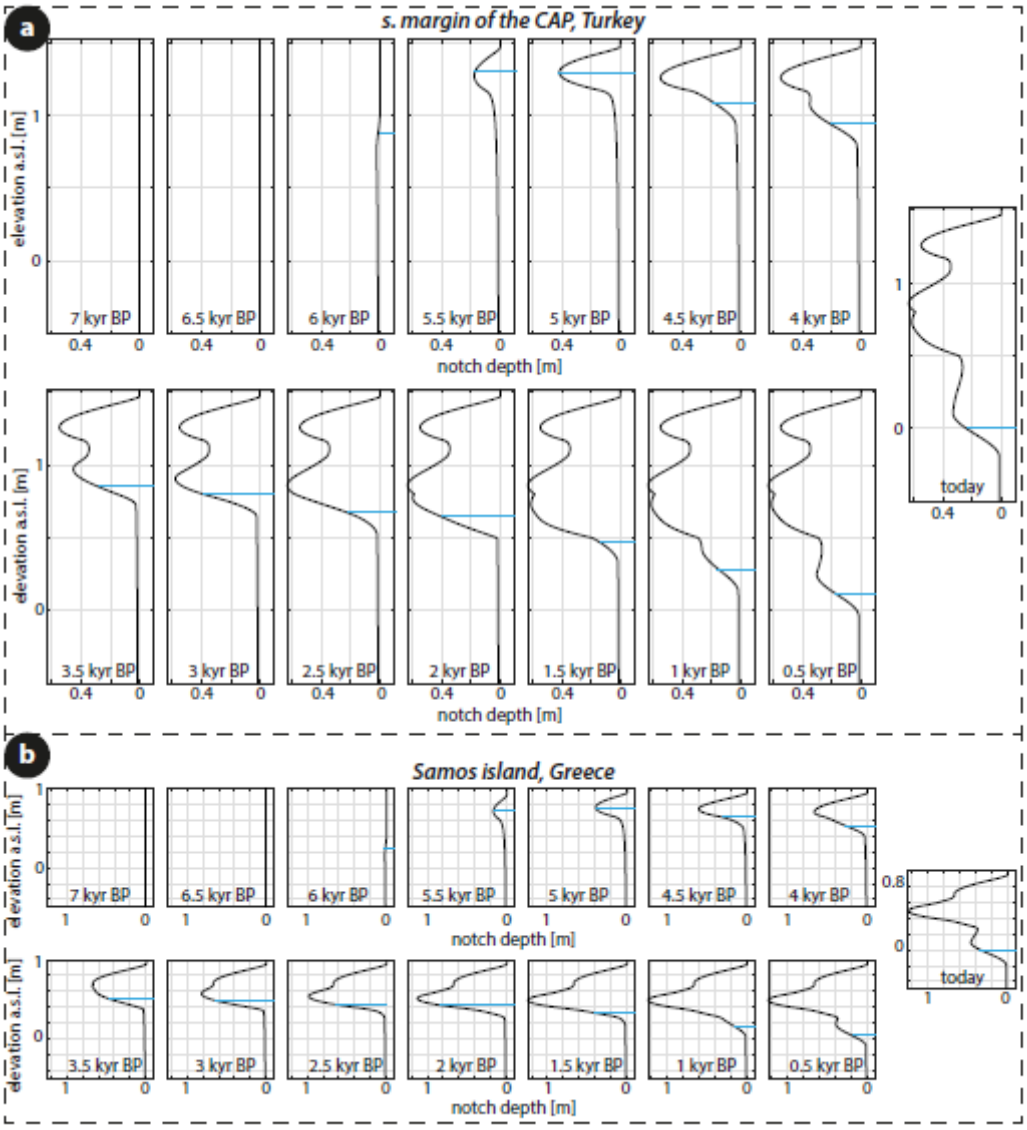


**Figure 9**. Time slices from tidal notch simulation in southern Turkey (a) and in the eastern Aegean Sea (b). Both regions are representative for coastlines emerging at significantly less than 1 mm/yr. Blue lines indicate sea-level at that time.

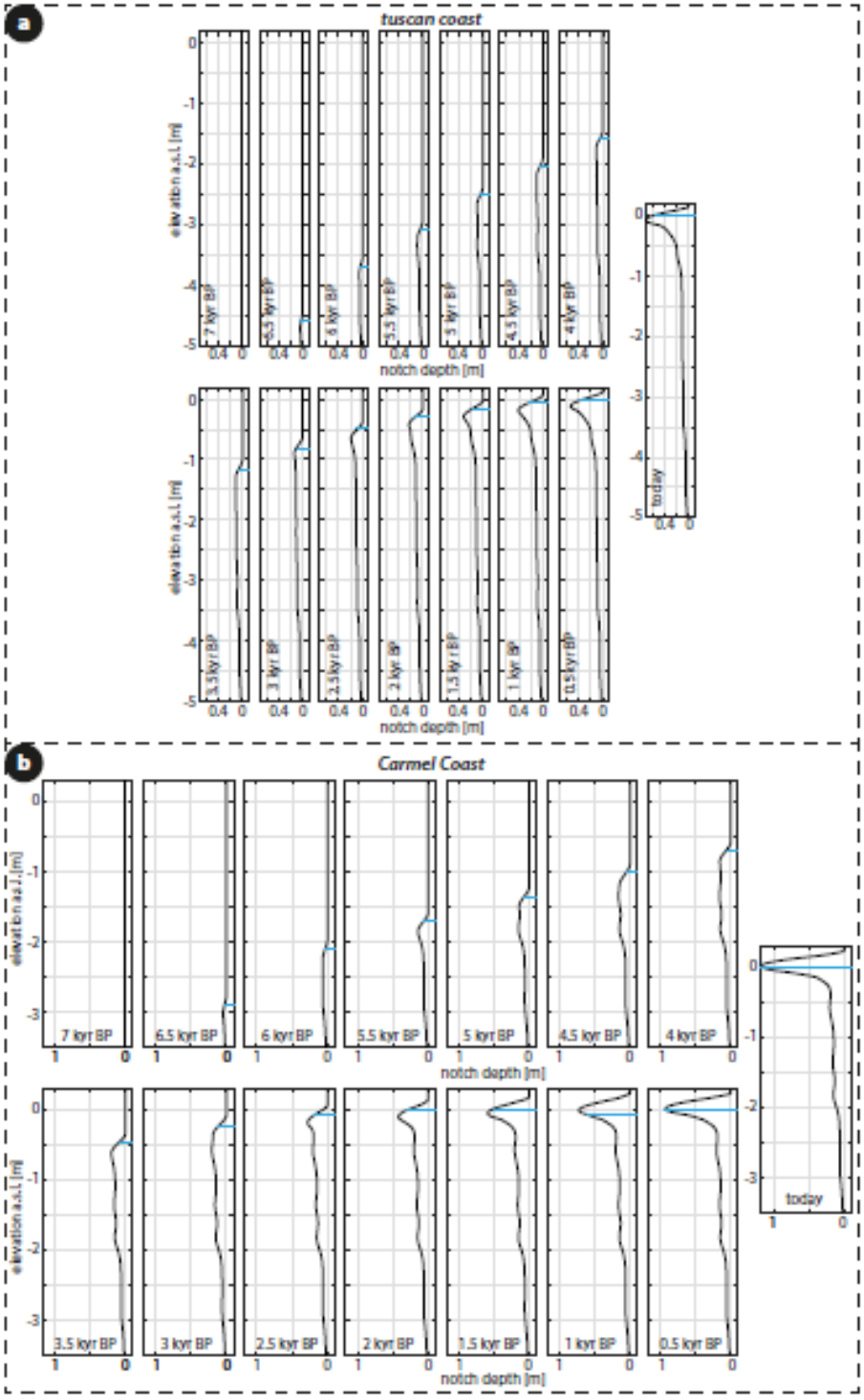


**Figure 10**. Time slices of Mid-Holocene notch development in tectonically stable regions. (a) northern Thyrrenian Sea, coast of Tuscany. (b) Carmel Coast, Isreal. Blue lines indicate sea-level at that time.

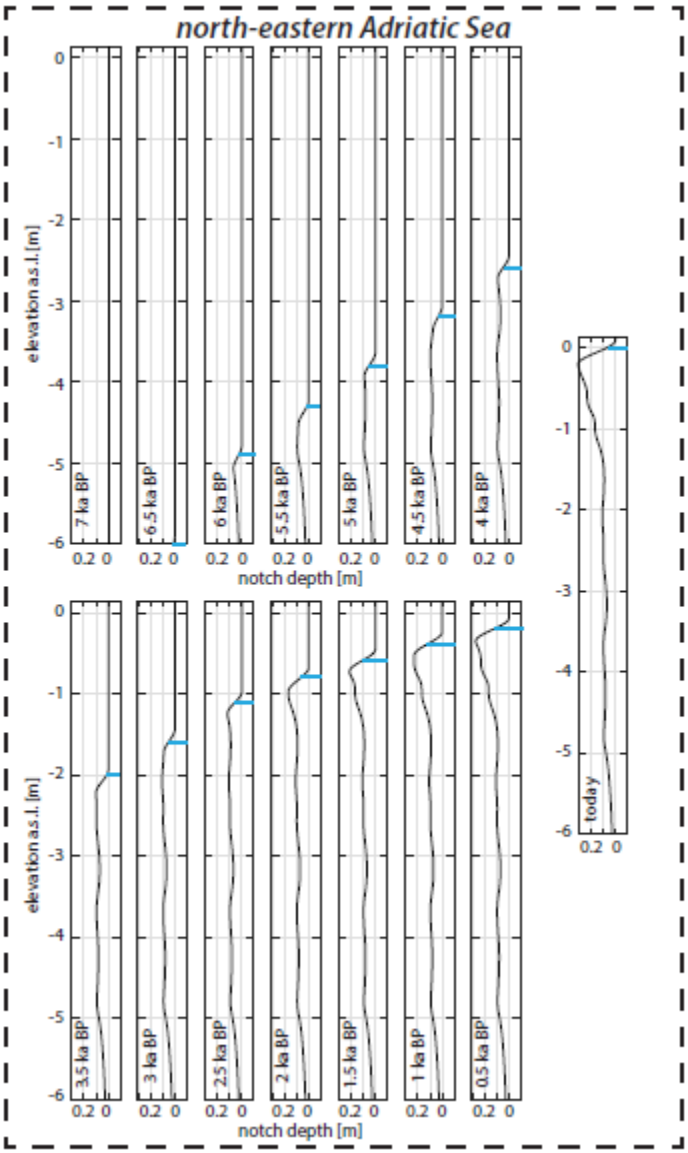


**Figure 11**. Modelled time slices of notch sequence development in subsiding regions. Blue lines indicate sea-level at that time.

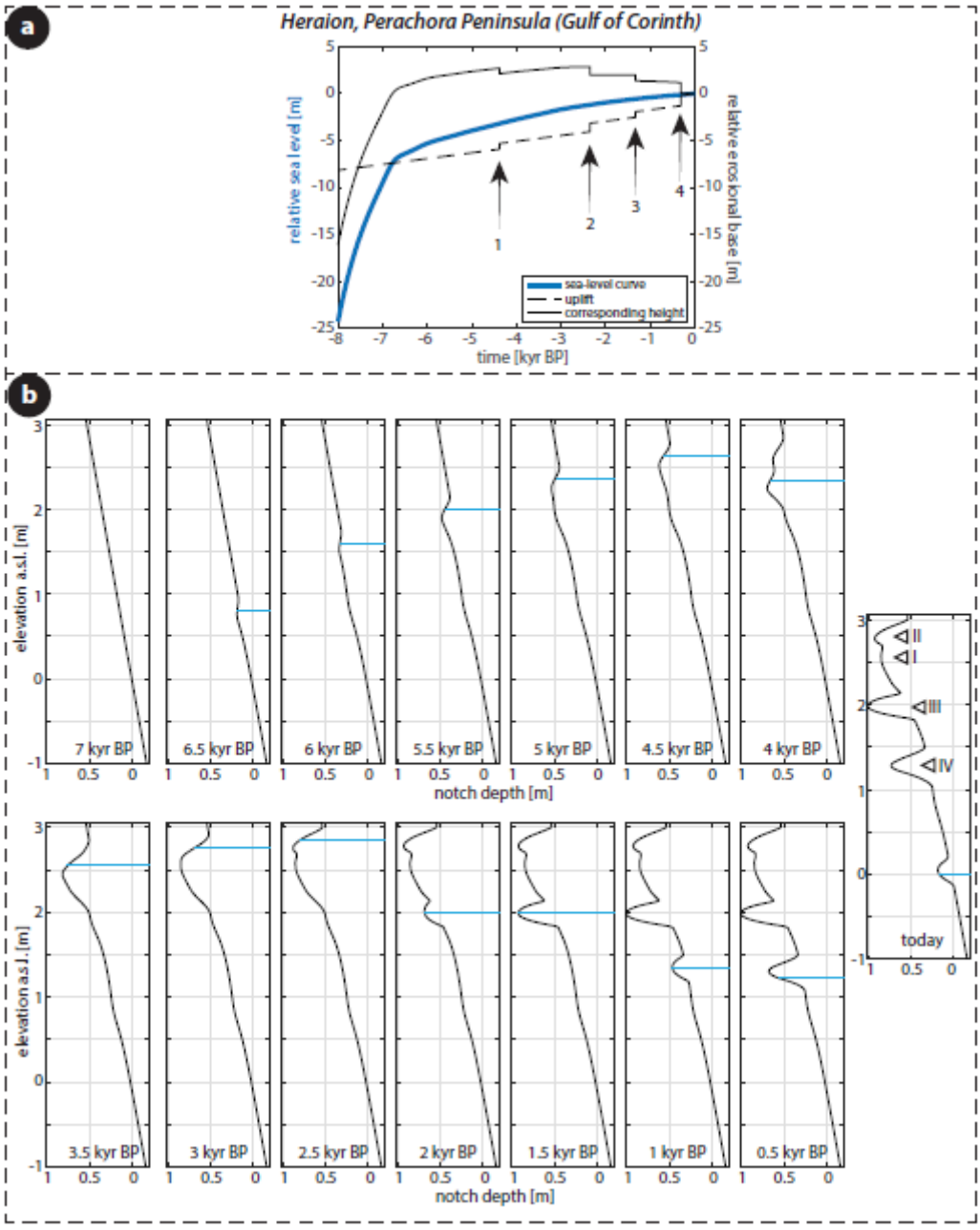


**Figure 12**. Results for the Heraion site in the eastern Gulf of Corinth including coseismic activity. a) Coseismically modified progression of the erosional base. Arrows refer to events listed in table 2. b) Modelled notch sequence evolution including coseismic uplifting events dated by or inferred from *Pirazzoli et al*. [1994]. Triangles indicate erosional features at corresponding mean sea-level on the modern cliff in between two coseismic uplift events. Blue lines indicate sea-level at that time.

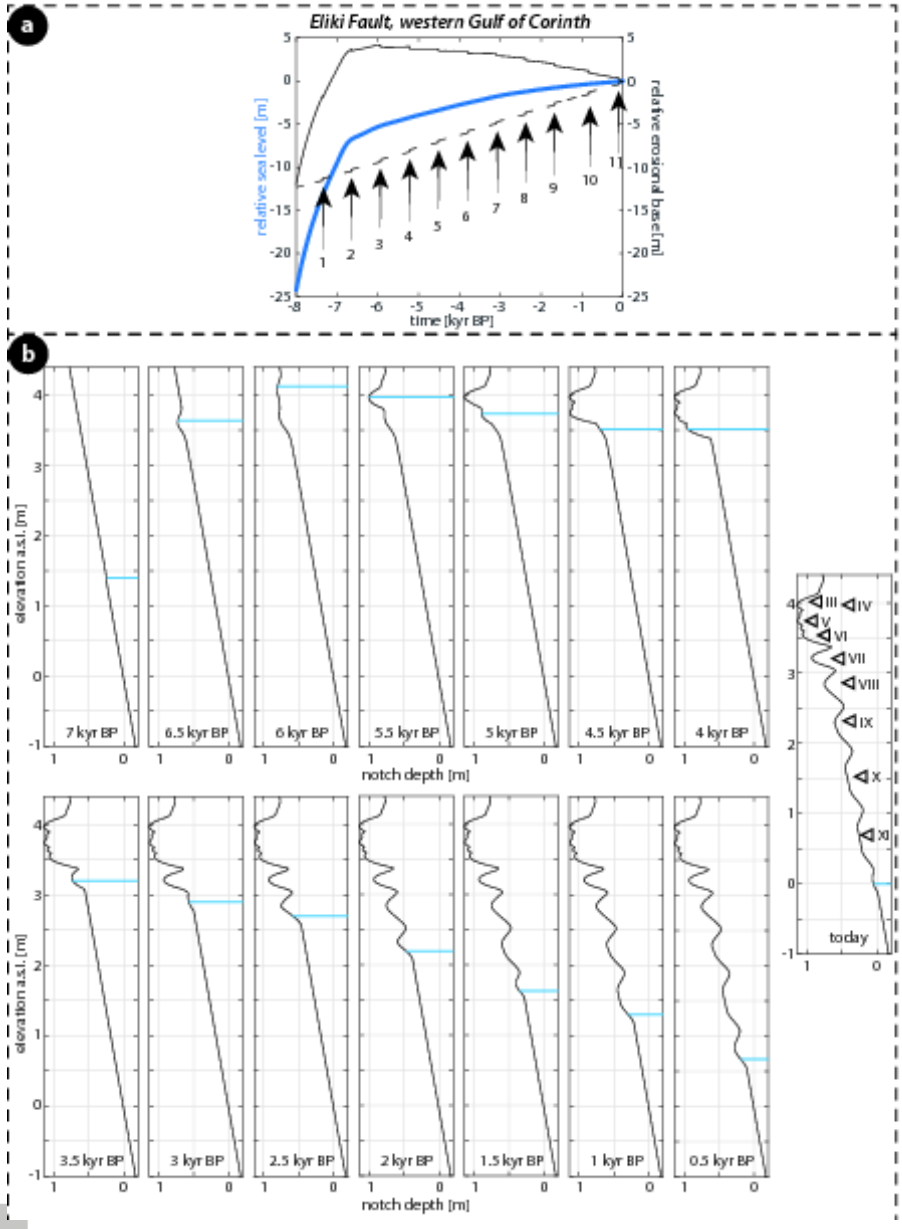


**Figure 13**. Results for the Eliki site in the western Gulf of Corinth including the coseismic activity of 11 events. a) showing the local sea-level curve and landmass evolution exhibiting coseismic uplifts. b) modelled time slices of cliff face evolution. Triangles indicate erosional features at corresponding mean sea-level on the modern cliff in between two coseismic uplift events. Blue lines indicate sea-level at that time.

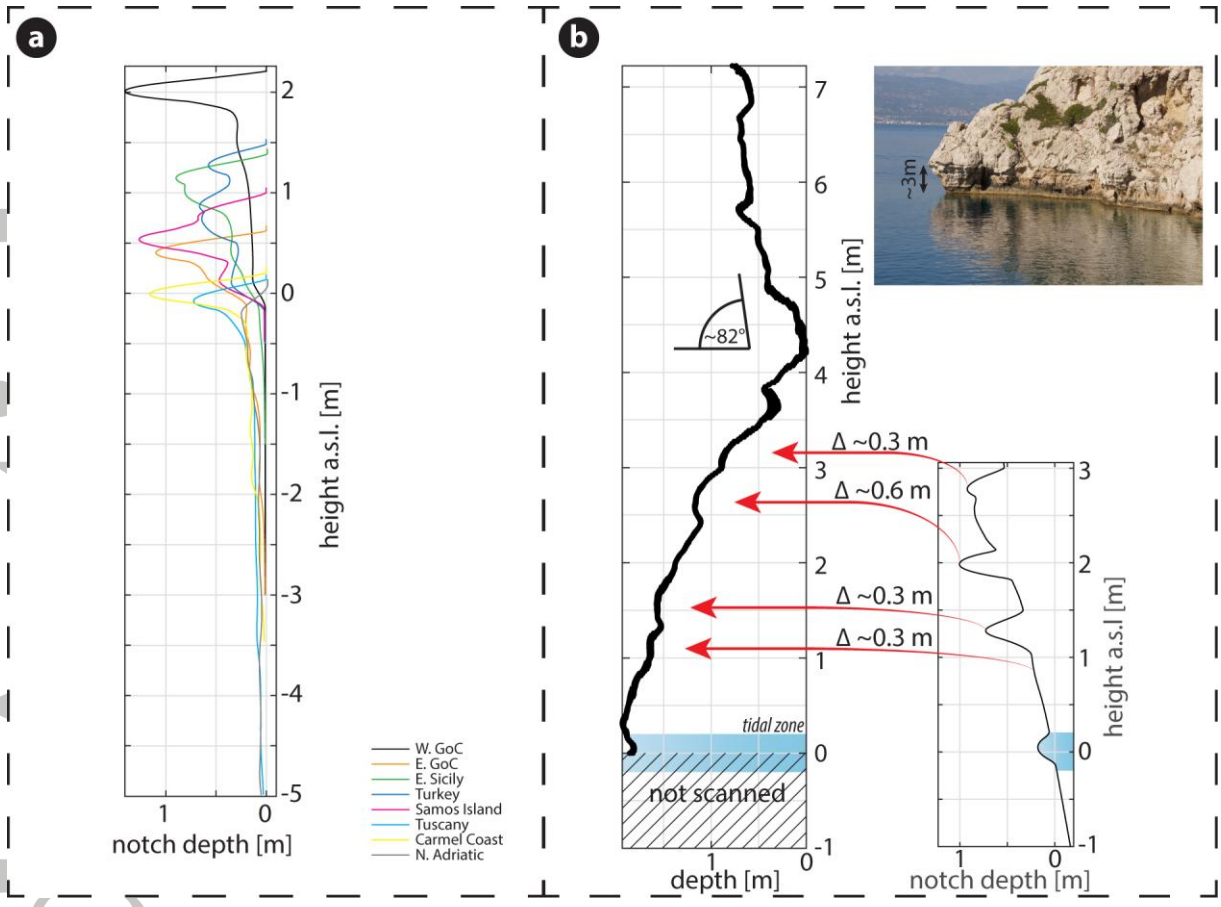


**Figure 14.** Comparing the model to reality. a) Comparison of all modelled notch profiles free from coseismic displacements. b) Comparison of modelled notch profile (E. Gulf of Corinth) containing coseismic uplifts to an actual notch profile extracted from TLS data at Cape Heraion, Perachora Peninsula [after *Schneiderwind et al.*, 2017].